PHSD-PHQMD code: unified Parton-Hadron-String Dynamics & Parton-Hadron-Quantum-Molecular Dynamics Transport approaches

User Guide

April 30, 2026

The PHSD-PHQMD Team

The code is available from:
https://phsd-phqmd.github.io/index.html

Contact E-mails:
phsd.phqmd@gmail.com

Table of content

Introduction

0.0.1 PHSD-PHQMD code

PHSD–PHQMD is a Fortran-based unified transport simulation framework for relativistic nucleus–nucleus collisions.

• It combines two complementary descriptions of baryon dynamics: **PHSD**, based on mean-field BUU transport, and **PHQMD**, which is a **Quantum Molecular Dynamics (QMD)** n-body approach.

• In both modes, the subsequent evolution includes partons (quarks, gluons) and mesons, propagated within a nonequilibrium Kadanoff–Baym or BUU dynamics.

• Interactions are handled through a collision integral for off-shell hadrons and QGP partons, realized within the **Dynamical-QuasiParti.**

• **Final-state nuclearcle Model (DQPM)** describing the partonic medium in line with lattice QCD (lQCD) thermodynamics fragments and formed clusters can be reconstructed with the **MST** (Minimum Spanning Tree), **SACA** (Simulated Annealing Cluster Algorithm), or **coalescence-based** algorithms.

• The simulated events are exported in **OSCAR**, **ROOT**, and **Rivet** formats.

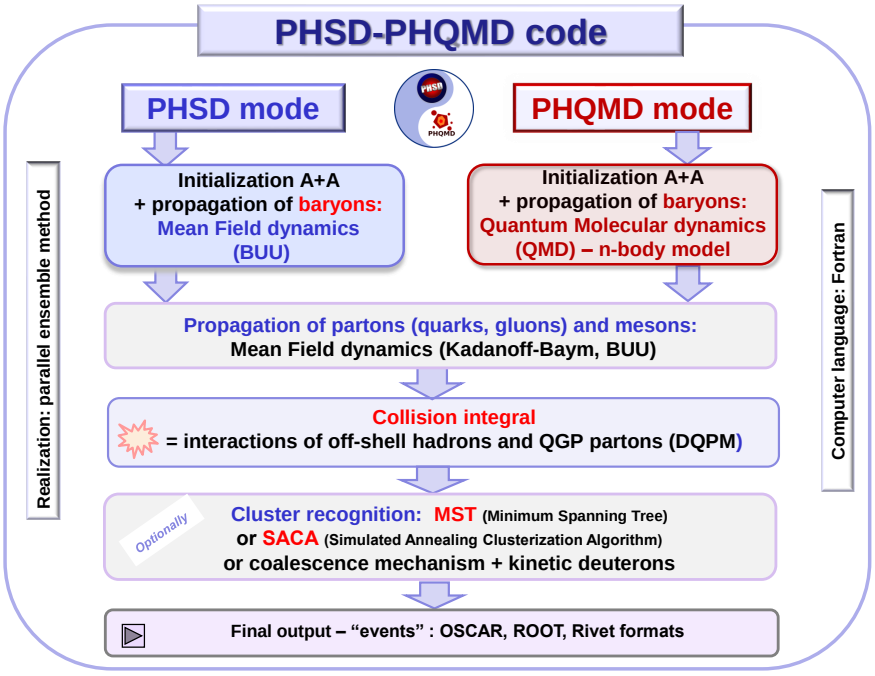

0.0.2 How to cite the PHSD-PHQMD code:

If you use the PHSD–PHQMD code in your scientific work, please cite it as
"PHSD–PHQMD code v.X.X in PHSD (or PHQMD) mode"
following the version numbering given on the PHSD–PHQMD web page:
https://phsd-phqmd.github.io/index.html

Please state explicitly which mode of the code has been used in your calculations and refer to the corresponding model name and provide respective citations, i.e.
- **PHSD mode**: the PHSD microscopic transport approach [1, 2, 3];
- **PHQMD mode**: the PHQMD microscopic transport approach [4, 5].

0.0.3 Parton-Hadron-String Dynamics (PHSD)

The **Parton-Hadron-String Dynamics** (PHSD) transport approach is a microscopic covariant dynamical approach for strongly interacting systems in and out-of equilibrium [1, 2, 6, 7, 8, 3]. The PHSD incorporates both partonic and hadronic degrees-of-freedom as well as the transition from the hadronic to the partonic phase, the QGP phase in terms of strongly interacting quasiparticles with further dynamical hadronization and final hadronic interactions in the late stage; thus, PHSD covers the full time evolution of a relativistic heavy-ion collision on a microscopic level. The dynamical description of the strongly interacting system is realized by solving the generalised off-shell Cassing's transport equations which are obtained from the Kadanoff-Baym equations [9, 10, 11] in first-order gradient expansion and go beyond the mean-field and on-shell Boltzmann approximation for the collision terms.

The theoretical description of the partonic degrees-of-freedom (quarks and gluons) is realized in line with the Dynamical-Quasi-Particle Model (DQPM) [12, 11, 3] and describes the properties of QCD in terms of resummed single-particle Green's functions. The three parameters of the DQPM are fitted to reproduce lQCD results in thermodynamical equilibrium [13, 14] such as energy density, pressure and entropy density; the real and imaginary parts of the parton self-energies are used to define the widths and pole positions of the spectral functions of quarks and gluons taken in Lorentzian form.

The DQPM provides the properties of the partons, i.e. masses and widths in their spectral functions as well as the mean fields for gluons/quarks and their effective 2-body interactions that are implemented in the PHSD. For details about the DQPM model and the off-shell transport approach we refer the reader to the reviews in Refs. [2, 8, 3]. We mention, that in equilibrium the PHSD reproduces the partonic transport coefficients – such as shear and bulk viscosities or the electric conductivity as well as diffusion coefficient matrix and charm spacial diffusion – from lattice QCD (lQCD) calculations as well [8, 15, 16, 17, 18].

The hadronic part is governed by the **Hadron-String-Dynamics** (HSD) part of the transport approach [19, 20]; the hadronic degrees-of-freedom include the baryon octet and decouplet, the 0^- and 1^- meson nonets as well as higher resonances. In the beginning of relativistic heavy-ion collisions color-neutral strings (described by the LUND model [21] using the FRITIOF 7.02 package (including PYTHIA and JETSET)) are produced in highly energetic scatterings of nucleons from the impinging nuclei, i.e. two strings can

form through primary NN collisions. These strings are dissolved into 'pre-hadrons', i.e. unformed hadrons with a formation time of $\tau_F \sim 0.8$ fm/c in the rest frame of the corresponding string, except for the 'leading hadrons'. Those are the fastest residues of the string ends, which can re-interact (practically instantly) with hadrons with a reduced cross sections in line with quark counting rules. If the energy density is below the critical value for the phase transition, which is taken to be $\mathcal{E}_C = 0.4\ GeV/fm^{-3}$ (e.g. in p+p reactions or in the hadronic corona), 'pre-hadrons' become real hadrons after the formation time $t_F = \tau_F\gamma$ (γ is the Lorentz gamma factor of the pre-hadron) in the calculational frame (center-of-mass system of A+A) and interact with hadronic cross sections. If the local energy density is larger than the critical value for the phase transition $\mathcal{E}_C$, the pre-hadrons melt into (colored) effective quarks and antiquarks in their self-generated repulsive mean-field as defined by the DQPM [2]. In the DQPM the quarks, antiquarks and gluons are dressed quasi-particles and have temperature-dependent effective masses and widths which have been fitted to lattice thermal quantities such as energy density, pressure and entropy density.

For the time evolution of the QGP phase off-shell transport equations with self-energies and cross-sections from the DQPM are used. With the expansion of the fireball the probability for the hadronization of partons increases strongly close to the phase boundary. The hadronisation is carried out on the basis of covariant transition rates. The resulting hadronic system is then governed by the off-shell HSD dynamics with optionally incorporated self-energies for the hadronic degrees-of-freedom [22].

To summarize: the full evolution of a relativistic heavy-ion collision, from the initial hard NN collisions out-of equilibrium up to the hadronisation and final interactions of the resulting hadronic particles is fully realized in the PHSD approach. We recall that PHSD has been successfully employed for p+p, p+A and A+A reactions ranging from SIS to LHC energies.

0.0.4 Parton-Hadron-Quantum-Molecular Dynamics (PHQMD)

The Parton-Hadron-Quantum-Molecular Dynamics (PHQMD) is an n-body transport approach designed to provide a microscopic description of nuclear cluster and hypernucleus formation as well as general particle production in heavy-ion reactions at relativistic energies. The PHQMD [4, 23, 24, 5, 25] combines the baryon propagation from the Quantum Molecular Dynamics (QMD) model [26, 27, 28, 29] with the dynamical properties and interactions of hadronic and partonic degrees-of-freedom from the Parton-Hadron-String-Dynamics (PHSD) approach [1, 2, 6, 7, 8, 3].

A novel development in PHQMD [30, 31] is the inclusion of a momentum-dependent nucleon potential in addition to the static, density-dependent Skyrme interaction. This enables three distinct EoS scenarios: two static ("soft" and "hard," differing in compressibility) and a soft, momentum-dependent EoS calibrated to pA elastic scattering data.

Cluster Production in PHQMD:

In difference to coalescence or statistical models, often used for cluster formation, PHQMD forms clusters dynamically due to interactions between baryons described on the basis of Quantum Molecular Dynamics, which allows for the propagation of the n-body Wigner density and n-body correlations in phase-space, essential for cluster formation.

Clusters can be identified in PHQMD using three different algorithms:

1. **Potential mechanism:** The attractive potential between baryons with a small relative momentum keeps them close together and can lead to a group of bound nucleons. Such groups of co-moving nucleons can be identified as clusters during the dynamical evolution, using the advanced Minimum Spanning Tree (aMST) method, as detailed in Ref. [5], or the SACA (Simulated Annealing Cluster Algorithm)[26], which finds the most bound configuration of nucleons and hyperons.
   MST [26] collects nucleons, which are close in coordinate space. At a given time t a snapshot of the positions and momenta of all nucleons is recorded and the MST clusterization algorithm is applied: two nucleons i and j are considered as "bound" to a deuteron or to a larger cluster $A > 2$ if they fulfill the condition

$$|\mathbf{r}_i^* - \mathbf{r}_j^*| < r_{clus} \,, \tag{0.0.1}$$

   where on the left hand side the positions are boosted in the center-of-mass of the ij pair. The maximal distance between cluster nucleons, $r_{clus} = 4$ fm, corresponds roughly to the range of the attractive NN potential. Additionally to MST, in aMST clusters must have negative binding energy $E_B < 0$. Moreover, aMST includes a stabilization algorithm to prevent spontaneous decay of clusters due to their semi-calssical treatment [5]. We note that (a)MST serves as a cluster recognition tool (applied in perturbative way) rather than a formation mechanism, since QMD propagates baryons, not pre-formed clusters.
2. **Kinetic mechanism:** Deuterons are created through catalytic hadronic reactions $\pi NN \leftrightarrow \pi d$ and $NNN \leftrightarrow Nd$ in different isospin channels. Quantum nature is considered via an excluded volume and the projection onto the deuteron wave function in momentum space, reducing production particularly at target/projectile rapidities. Details are given in Ref. [5].
3. **Coalescence mechanism:** A proton and neutron form a deuteron if their phase-space distance at freeze-out satisfies $|r_1 - r_2| \leq 3.575$ fm and $|p_1 - p_2| \leq 285$ MeV/c. Details are given in Ref. [24]. This (perturbative) method is used in the PHQMD for model studies and comparison purposes only.

Chapter 1

Technical information

1.1 Files description & code structure

The PHSD-PHQMD code is a unified framework for the microscopic description of heavy-ion (A+A), proton-induced reactions (p+A and p+p) as well as pion-induced reactions (pi+A, pi+N). The solution of transport equations is based on the parallel ensemble method for both PHSD and PHQMD modes.

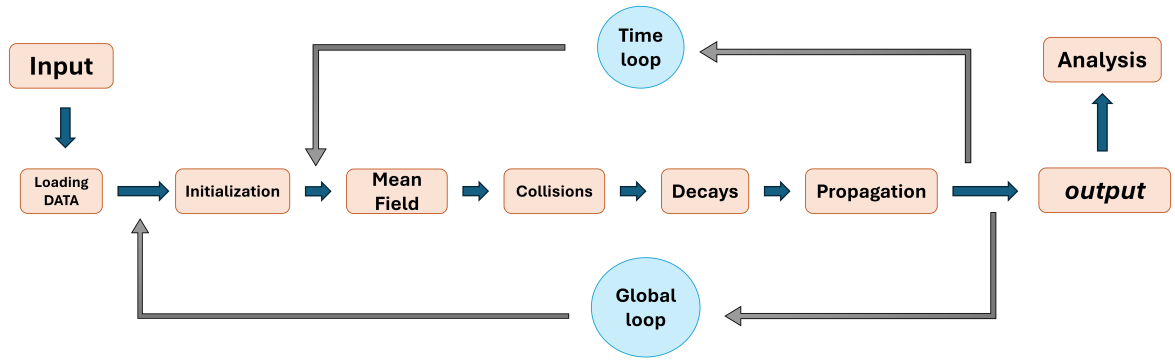

Global loop over:

- the impact parameter b (if one runs over different `b` values),
- the subsequent runs `ISUB`,
- and the parallel events `NUM` (which describe the quantum aspect of the reaction).

The interaction between particles is allowed only inside a single event (but is allowed between parallel events for hadronization).

1.2 Compiling and running the code

The minimum requirement to compile the PHSD–PHQMD code is a Fortran 90 compiler running under Linux, Windows, or macOS platforms (32 or 64 bit). On Linux, the build system uses *CMake* (version $\geq$ 3.15), while on Windows batch build scripts are provided. The recommended compilers for PHSD–PHQMD are the **GFortran compiler**, **Intel Fortran Compiler** (*ifort*), and **Intel LLVM Fortran Compiler** (*ifx*).

Compilation on Linux

On Linux, the code is compiled out-of-source using *CMake*. In the top source directory, create a separate build directory and run:

```
$ mkdir build
$ cd build
$ cmake -DCMAKE_BUILD_TYPE=Release ..
$ make
```

By default, *gfortran* is used as the Fortran compiler. If supported by the compiler and platform, link-time optimization is enabled automatically.

To compile with the Intel Fortran compiler (*ifort*), use:

```
$ cmake -DCMAKE_Fortran_COMPILER=ifort -DCMAKE_BUILD_TYPE=
   Release ..
$ make
```

To compile with the Intel LLVM Fortran compiler (*ifx*), use:

```
$ cmake -DCMAKE_Fortran_COMPILER=ifx -DCMAKE_BUILD_TYPE=
   Release ..
$ make
```

If supported, interprocedural optimization is enabled automatically for Intel compilers.

LHC energies:
To run the code at LHC energies, it is mandatory to compile the code in **double precision mode**. For all supported Linux compilers (*gfortran*, *ifort*, *ifx*), this is done with:

```
$ cmake -DCMAKE_BUILD_TYPE=ReleaseR8 ..
$ make
```

For debugging, omit *-DCMAKE_BUILD_TYPE* or explicitly use:

```
$ cmake -DCMAKE_BUILD_TYPE=Debug ..
$ make
```

Compilation on Windows

On Windows, the code has been tested with *f90* from Compaq Fortran 6.x. Several batch files are provided in order to simplify the build procedure:

- *make.bat*: builds the executable file *phsd.exe*,
- *make_clean.bat*: removes generated files,
- *make_debug.bat*: builds the debug version,
- *make_LHC.bat*: builds the code in double precision mode for LHC energies.

After successful compilation the executable file has the name *phsd.exe*. The following terminal display the full procedure:

```
$ unzip PHSD_PHQMD_versionXXX.zip -d phsd-phqmd/
$ cd phsd-phqmd/
$ make
$ ./phsd.exe
```

Running the PHSD–PHQMD code

For execution, the input file *inputPHSD* and the directory *INPUT_DATA* are mandatory. A convenient way to run the code is to create a separate run directory in the top source directory and link or copy the required files:

```
$ mkdir test_run
$ cd test_run
$ ln -s ../build/phsd .
$ ln -s ../INPUT_DATA .
$ cp ../inputPHSD .
$ ./phsd
```

This procedure keeps the build directory and the run directory separate, which is recommended for production runs and testing.

1.2.1 PHSD and PHQMD modes

The code can be run in two modes: **PHSD** and **PHQMD**. This is controlled by the flag `IPHQMD` in the `inputPHSD` file:

- `IPHQMD = 0`: PHSD dynamics
- `IPHQMD = 1`: propagation with QMD dynamics

The PHSD mode can be used for heavy-ion $A + A$, proton induced reactions $p + A$, $p + p$ reactions, for pion induced reactions $\pi^- + A$ and $\pi^- + p$ as well as for anti-proton induced reactions $\bar{p} + A$ and $\bar{p} + A$. For anti-proton induced initialization please contact the PHSD-PHQMD Team for special instructions.

The PHQMD mode can be used for heavy-ion $A + A$ and proton induced reactions $p + A$, $p + p$.

Both modes (in default settings) include the QGP stage with partonic degrees-of-freedom and their interactions. However, one can run the code without QGP (for model studies). This is controled by the parameter IGLUE in `inputPHSD` (see below).

1.3 Particle identification

The baryons and mesons are stored in two different vectors:

Baryons:

ID(i,1) - type of baryon i

ID(i,2) - electric charge of baryon i

Antibaryons carry the ID(i,1) with negative sign.

Mesons:

IPI(j,1) - type of meson j

IPI(j,2) - electric charge of meson j

* For broad resonances the mass is indicated by the pole of the spectral function.

1.3.1 Baryons

The PHSD-PHQMD approach incorporates nucleons, Δ's, N*(1440), N*(1535), Λ, Σ and Σ^* hyperons, Ξ's, Ξ^*'s and Ω's as well as their antiparticles on the baryonic side and the 0^- and 1^- octet states in the mesonic sector.

Higher baryonic resonances are discarded as explicit states (for propagation) in PHSD-PHQMD; they are supposed to "melt" in the nuclear medium even at normal nuclear density (see e.g. [32, 33, 34]). The argument here is that the resonance structure (above the Δ-peak) is not seen experimentally even in photoabsorption on light nuclei [35, 36, 37].

Table 1.1: The **baryon** identification codes. Light baryons

ID(j,1)	ID(j,2)	type	ID(PDG)	mass* [GeV]
1	1	p	2212	0.938
1	0	n	2112	0.938
2	-1	Δ^-	1114	1.232
2	0	Δ^0	2114	1.232
2	+1	Δ^+	2214	1.232
2	+2	Δ^{++}	2224	1.232
3	0	N(1440)^0	2112	1.440
3	+1	N(1440)$^+$	2212	1.440
4	0	N(1535)^0	2112	1.535
4	+1	N(1535)$^+$	2212	1.535

Example: p : ID(j,1) $= 1$, ID(j,2) $= +1$; $\bar{p}$: ID(j,1) $= -1$, ID(j,2) $= -1$

Table 1.2: The **baryon** identification codes. Strange baryons

ID(j,1)	ID(j,2)	type	ID(PDG)	mass* [GeV]
5	0	Λ	3122	1.115
6	-1	Σ^-	3112	1.189
6	0	Σ^0	3212	1.189
6	+1	Σ^+	3222	1.189
7	-1	Σ^{*-}	3114	1.385
7	0	Σ^{*0}	3214	1.385
7	+1	Σ^{*+}	3224	1.385
8	-1	Ξ^-	3312	1.314
8	0	Ξ^0	3322	1.314
9	-1	Ξ^{*-}	3314	1.530
9	0	Ξ^{*0}	3324	1.530
10	-1	Ω^-	3334	1.672

Table 1.3: The **baryon** identification codes. Charmed baryons

ID(j,1)	ID(j,2)	type	ID(PDG)	mass* [GeV]
11	+1	Λ_c^+	4122	2.286
12	0	Σ_c^0	4112	2.455
12	+1	Σ_c^+	4212	2.455
12	+2	Σ_c^{++}	4222	2.455
13	0	Ξ_c^0	4132	2.467
13	+1	Ξ_c^+	4232	2.467
14	0	Σ_c^{*0}	4114	2.517
14	+1	Σ_c^{*+}	4214	2.517
14	+2	Σ_c^{*++}	4224	2.517
15	-	-	-	-
16	0	$\Xi_c^{\prime 0}$	4312	2.575
16	+1	$\Xi_c^{\prime +}$	4322	2.575
17	0	Ξ_c^{*0}	4314	2.63
17	+1	Ξ_c^{*+}	4324	2.63
18	0	Ω_c^0	4332	2.695
19	0	Ω_c^{*0}	4334	2.765

Table 1.4: The **baryon** identification codes. Bottom baryons

ID(j,1)	ID(j,2)	type	ID(PDG)	mass* [GeV]
20	0	Λ_b^0	5122	5.620
21	-1	Σ_b^-	5112	5.807
21	0	Σ_b^0	5212	5.807
21	+1	Σ_b^+	5222	5.807
22	-1	Σ_b^{*-}	5114	5.829
22	0	Σ_b^{*0}	5214	5.829
22	+1	Σ_b^{*+}	5224	5.829

Table 1.5: The **meson** identification codes. Light mesons

IPI(j,1)	IPI(j,2)	type	ID(PDG)	mass* [GeV]
1	+1	π^+	211	0.138
1	0	π^0	111	0.138
1	-1	π^-	-211	0.138
2	0	η	221	0.549
3	+1	K^+	321	0.494
3	-1	K^-	-321	0.494
4	+1	K^{*+}	323	0.892
4	-1	K^{*-}	-323	0.892
5	-1	ρ^-	-213	0.770
5	0	ρ^0	113	0.770
5	+1	ρ^+	213	0.770
6	0	$\omega(783)$	223	0.782
7	0	$\phi(1020)$	333	1.020
8	0	η'	331	0.958
9	-1	a_1^-	-20213	1.230
9	0	a_1^0	20113	1.230
9	+1	a_1^+	20213	1.230
11	0	K^0	311	0.494
12	0	$\bar{K}^0$	-311	0.494
13	0	K^{*0}	313	0.892
14	0	$\bar{K}^{*0}$	-313	0.892

1.3.2 Mesons

Table 1.6: The **meson** identification codes. Charm mesons

IPI(j,1)	IPI(j,2)	type	ID(PDG)	mass* [GeV]
10	0	J/ψ	443	3.097
15	+1	D^+	411	1.870
15	-1	D^-	-411	1.870
16	0	D^0	421	1.865
17	0	$\bar{D}^0$	-421	1.865
18	+1	$D^{*+}(2010)$	413	2.010
18	-1	$D^{*-}(2010)$	-413	2.010
19	0	$D^{*0}(2007)$	423	2.007
20	0	$\bar{D}^{*0}(2007)$	-423	2.007
22	0	ψ'	100443	3.686
23	+1	D_s^+	431	1.968
24	-1	D_s^-	-431	1.968
25	+1	$D_s^{*+}(2112)$	433	2.112
26	-1	$D_s^{*-}(2112)$	-433	2.112
27	0	η_c	441	2.980
28	0	$\chi_{c0}(1P)$	10441	3.415
29	0	$\chi_{c1}(1P)$	20443	3.511
30	0	$\chi_{c2}(1P)$	445	3.556

Example: π^+ : IPI(j,1) = 1, IPI(j,2) = +1 ; π^- : IPI(j,1) = 1, IPI(j,2) = −1

Table 1.7: The **meson** identification codes. Bottom mesons

IPI(j,1)	IPI(j,2)	type	ID(PDG)	mass* [GeV]
31	+1	B^+	521	5.279
31	-1	B^-	-521	5.279
32	0	B^0	511	5.279
33	0	$\bar{B}^0$	-511	5.279
34	+1	B^{*+}	523	5.279
34	-1	B^{*-}	-523	5.279
35	0	B^{*0}	513	5.325
36	0	$\bar{B}^{*0}$	-513	5.325
37	0	B_s^0	531	5.366
38	0	$\bar{B}_s^0$	-531	5.366
39	0	B_s^{*0}	533	5.415
40	0	$\bar{B}_s^{*0}$	-533	5.415
41	+1	B_c^{*+}	543	6.602
41	-1	B_c^{*-}	-543	6.602

Table 1.8: The **meson** identification codes. Bottomonia

IPI(j,1)	IPI(j,2)	type	ID(PDG)	mass* [GeV]
42	0	$\Upsilon(1S)$	553	9.460
43	0	$\chi_{b0}(1P)$	10551	9.859
44	0	$\chi_{b1}(1P)$	20553	9.893
45	0	$\chi_{b2}(1P)$	555	9.912
46	0	$\Upsilon(2S)$	100553	10.023
47	0	$\chi_{b0}(2P)$	110551	10.233
48	0	$\chi_{b1}(2P)$	120553	10.255
49	-	-	-	-
50	0	$\chi_{b2}(2P)$	100555	10.269
51	0	$\Upsilon(3S)$	200553	10.355

1.4 Input files and initialization options

1.4.1 Input file *inputPHSD* and options

To run the PHSD–PHQMD code, the user must specify both the **initial setup** of the collision and the **initial parameters** that control the simulation options. The **initial setup** includes the collision system, beam energy, and centrality class. The **initial parameters** determine the operational mode of the code, such as whether the simulation is performed in PHSD or PHQMD mode, whether the QGP phase is included, and whether medium effects for hadrons are taken into account. All these parameters must be defined in the input file *inputPHSD*.

The file *inputPHSD* must be located in the main code directory together with the executable file `phsd.exe`. Several example versions of the *inputPHSD* file are provided in the main code directory and may serve as templates for constructing new input configurations.

At the start of the program execution, the *inputPHSD* file is read by the `main` routine and the parameters are checked for consistency. If any parameter is specified incorrectly, the program will terminate during the initialization stage. In such cases, the corresponding error message can be found in the file `fort.80` or in the working log file.

In addition, the directory `/INPUT_DATA/` must be present in the main code directory. This directory contains tabulated input data required by the simulation, including the G-matrix amplitudes for channels with strangeness, tabulated charm production cross sections, and data files with tabulated cross sections for Δ resonance scattering and other processes. When organizing multiple job submissions (e.g. in batch systems), it is important to ensure that each job has proper access to the `/INPUT_DATA/` directory.

Further internal parameters and initialization options are defined in the file `ini_param.f`. Default values are specified in this file, and modifications are generally discouraged unless discussed with the code authors, as they may affect the physical consistency of the simulation.

The program execution begins with reading the *inputPHSD* file followed by the initialization procedures. During initialization, the partonic cross sections are pre-calculated and stored in multidimensional arrays. During the time evolution of the simulation, the code prints status messages to the screen or to a log file at each time step, for example:

```
PHSD runs at ISUB=   1     b [fm]= 2.25     time [fm/c]=   1.345997
PHSD runs at ISUB=   1     b [fm]= 2.25     time [fm/c]=   1.400159
PHSD runs at ISUB=   1     b [fm]= 2.25     time [fm/c]=   1.454321
PHSD runs at ISUB=   1     b [fm]= 2.25     time [fm/c]=   1.508483
PHSD runs at ISUB=   1     b [fm]= 2.25     time [fm/c]=   1.562645
```

Here we show how to initialize the code for A+A, p+p collisions as well as for π^-+A and π^-+p reactions. The flags in example files are shown for the PHSD mode, however, the activation of PHQMD mode is discussed below.

inputPHSD **for Au+Au,** $\sqrt{s_{NN}} = 200$ **GeV, 0-40%, PHSD mode**

197,	MASSTA:	target mass
79,	MSTAPR:	protons in target
197,	MASSPR:	projectile mass
79,	MSPRPR:	protons in projectile
21300.,	Tkin:	kinetic energy per nucleon in lab. frame in AGeV
0.0,	BMIN:	minimal impact parameter [fm] (no effect for p+A)
8.0,	BMAX:	maximal impact parameter [fm] (no effect for p+A)
0.5,	DeltaB:	step Δb in impact parameter [fm]
		(used only if IBweight_MC=0)
30,	NUM:	optimized number of parallel ensembles ("events")
1,	ISUBS:	number of subsequent runs ("events")
99999,	ISEED:	any integer number
1,	IGLUE:	=1 with partonic QGP phase;
		=0 - without QGP (HSD mode)
100.,	FINALT:	final time of calculation [fm/c]
		(if set =0, it will be computed in the PHSD)
11,	ILOW:	output level (default=11)
0,	Idilept:	=0 no dileptons; =1 electron pair; =2 muon pair
0,	ICQ:	=0 free spectral functions for vectar mesons,
		=1 drop. mass, =2 broadening, =3 drop.+broad.
0,	IHARD:	=1 with charm and bottom; =0 - without
0,	IBweight_MC:	=0 constant step in B =DBIMP;
		=1 choose B by Monte-Carlo ISUBS times
		in interval [Bmin,Bmax]
0,	INUCLEI:	=1 reactions with kinetic deuterons
0,	**IPHQMD:**	=1: propagation with QMD dynamics;
		=0 with HSD/PHSD dynamics
		(flags below are used for IPHQMD=1 only)
0,	iqmdeos:	EoS for QMD mode :
		=0: hard static EOS;
		=1 soft static EoS;
		=2 soft EoS with mom. dep.endence
0,	ISACA:	enable or disable SACA output
		(note: SACA or MST is controlled by iflagsaca)
10.0,	TSACA:	starting time for SACA
5.0,	DTSACA:	time step for SACA calculations
25,	NTSACA:	Number of SACA timesteps
		(tmax=tsaca+dtsaca·ntsaca must be < FINALT)
0,	iflagsaca:	=1 SACA (and MST), =0 MST only, no SACA

inputPHSD **for Au+Au,** $\sqrt{s_{NN}} = 200$ **GeV, 0-40%, PHQMD mode**

197,	MASSTA:	target mass
79,	MSTAPR:	protons in target
197,	MASSPR:	projectile mass
79,	MSPRPR:	protons in projectile
21300.,	Tkin:	kinetic energy per nucleon in lab. frame in AGeV
0.0,	BMIN:	minimal impact parameter [fm] (no effect for p+A)
8.0,	BMAX:	maximal impact parameter [fm] (no effect for p+A)
0.5,	DeltaB:	step Δb in impact parameter [fm]
		(used only if IBweight_MC=0)
30,	NUM:	optimized number of parallel ensembles ("events")
1,	ISUBS:	number of subsequent runs ("events")
99999,	ISEED:	any integer number
1,	IGLUE:	=1 with partonic QGP phase;
		=0 - without QGP (HSD mode)
140.,	FINALT:	final time of calculation [fm/c]
		(if set =0, it will be computed in the PHSD)
11,	ILOW:	output level (default=11)
0,	Idilept:	=0 no dileptons; =1 electron pair; =2 muon pair
0,	ICQ:	=0 free spectral functions for vectar mesons,
		=1 drop. mass, =2 broadening, =3 drop.+broad.
0,	IHARD:	=1 with charm and bottom; =0 - without
0,	IBweight_MC:	=0 constant step in B =DBIMP;
		=1 choose B by Monte-Carlo ISUBS times
		in interval [Bmin,Bmax]
1,	INUCLEI:	=1 reactions with kinetic deuterons
1,	**IPHQMD:**	=1: propagation with QMD dynamics;
		=0 with HSD/PHSD dynamics
		(flags below are used for IPHQMD=1 only)
0,	iqmdeos:	EoS for QMD mode :
		=0: hard static EOS;
		=1 soft static EoS;
		=2 soft EoS with mom. dep.endence
1,	ISACA:	enable or disable SACA output
		(note: SACA or MST is controlled by iflagsaca)
10.0,	TSACA:	starting time for SACA
5.0,	DTSACA:	time step for SACA calculations
25,	NTSACA:	Number of SACA timesteps
		(tmax=tsaca+dtsaca·ntsaca must be < FINALT)
0,	iflagsaca:	=1 SACA (and MST), =0 MST only, no SACA

inputPHSD **for** $p+p$**,** $\sqrt{s_{NN}} = 200$ **GeV**

1,	MASSTA:	target mass
1,	MSTAPR:	protons in target
1,	MASSPR:	projectile mass
1,	MSPRPR:	protons in projectile
21300.,	Tkin:	kinetic energy per nucleon in lab. frame in AGeV
0.0,	BMIN:	minimal impact parameter [fm] (no effect for p+A)
0.0,	BMAX:	maximal impact parameter [fm] (no effect for p+A)
0.5,	DeltaB:	step Δb in impact parameter [fm]
		(used only if IBweight_MC=0)
1000,	NUM:	optimized number of parallel ensembles ("events")
1,	ISUBS:	number of subsequent runs ("events")
99999,	ISEED:	any integer number
1,	IGLUE:	=1 with partonic QGP phase;
		=0 - without QGP (HSD mode)
60.,	FINALT:	final time of calculation [fm/c]
		(if set =0, it will be computed in the PHSD)
11,	ILOW:	output level (default=11)
0,	Idilept:	=0 no dileptons; =1 electron pair; =2 muon pair
0,	ICQ:	=0 free spectral functions for vectar mesons,
		=1 drop. mass, =2 broadening, =3 drop.+broad.
0,	IHARD:	=1 with charm and bottom; =0 - without
0,	IBweight_MC:	=0 constant step in B =DBIMP;
		=1 choose B by Monte-Carlo ISUBS times
		in interval [Bmin,Bmax]
0,	INUCLEI:	=1 reactions with kinetic deuterons
0,	**IPHQMD:**	=1: propagation with QMD dynamics;
		=0 with HSD/PHSD dynamics
		(flags below are used for IPHQMD=1 only)
0,	iqmdeos:	EoS for QMD mode :
		=0: hard static EOS;
		=1 soft static EoS;
		=2 soft EoS with mom. dep.endence
0,	ISACA:	enable or disable SACA output
		(note: SACA or MST is controlled by iflagsaca)
10.0,	TSACA:	starting time for SACA
5.0,	DTSACA:	time step for SACA calculations
25,	NTSACA:	Number of SACA timesteps
		(tmax=tsaca+dtsaca·ntsaca must be < FINALT)
0,	iflagsaca:	=1 SACA (and MST), =0 MST only, no SACA

inputPHSD **for π^-+Pb, 1.3 AGeV**

208,	MASSTA:	target mass
82,	MSTAPR:	protons in target
0,	MASSPR:	projectile mass
0,	MSPRPR:	protons in projectile
1.3,	Tkin:	kinetic energy per nucleon in lab. frame in AGeV
0.0,	BMIN:	minimal impact parameter [fm] (no effect for p+A)
0.0,	BMAX:	maximal impact parameter [fm] (no effect for p+A)
0.5,	DeltaB:	step Δb in impact parameter [fm]
		(used only if IBweight_MC=0)
1000,	NUM:	optimized number of parallel ensembles ("events")
1,	ISUBS:	number of subsequent runs ("events")
99999,	ISEED:	any integer number
1,	IGLUE:	=1 with partonic QGP phase;
		=0 - without QGP (HSD mode)
120.,	FINALT:	final time of calculation [fm/c]
		(if set =0, it will be computed in the PHSD)
11,	ILOW:	output level (default=11)
0,	Idilept:	=0 no dileptons; =1 electron pair; =2 muon pair
0,	ICQ:	=0 free spectral functions for vectar mesons,
		=1 drop. mass, =2 broadening, =3 drop.+broad.
0,	IHARD:	=1 with charm and bottom; =0 - without
0,	IBweight_MC:	=0 constant step in B =DBIMP;
		=1 choose B by Monte-Carlo ISUBS times
		in interval [Bmin,Bmax]
0,	INUCLEI:	=1 reactions with kinetic deuterons
0,	**IPHQMD:**	=1: propagation with QMD dynamics;
		=0 with HSD/PHSD dynamics
		(flags below are used for IPHQMD=1 only)
0,	iqmdeos:	EoS for QMD mode :
		=0: hard static EOS;
		=1 soft static EoS;
		=2 soft EoS with mom. dep.endence
0,	ISACA:	enable or disable SACA output
		(note: SACA or MST is controlled by iflagsaca)
10.0,	TSACA:	starting time for SACA
5.0,	DTSACA:	time step for SACA calculations
25,	NTSACA:	Number of SACA timesteps
		(tmax=tsaca+dtsaca·ntsaca must be < FINALT)
0,	iflagsaca:	=1 SACA (and MST), =0 MST only, no SACA

inputPHSD **for π^-+p, 1.3 AGeV**

1,	MASSTA:	target mass
1,	MSTAPR:	protons in target
0,	MASSPR:	projectile mass
0,	MSPRPR:	protons in projectile
1.3,	Tkin:	kinetic energy per nucleon in lab. frame in AGeV
0.0,	BMIN:	minimal impact parameter [fm] (no effect for p+A)
0.0,	BMAX:	maximal impact parameter [fm] (no effect for p+A)
0.5,	DeltaB:	step Δb in impact parameter [fm]
		(used only if IBweight_MC=0)
1000,	NUM:	optimized number of parallel ensembles ("events")
1,	ISUBS:	number of subsequent runs ("events")
99999,	ISEED:	any integer number
0,	IGLUE:	=1 with partonic QGP phase;
		=0 - without QGP (HSD mode)
120.,	FINALT:	final time of calculation [fm/c]
		(if set =0, it will be computed in the PHSD)
11,	ILOW:	output level (default=11)
0,	Idilept:	=0 no dileptons; =1 electron pair; =2 muon pair
0,	ICQ:	=0 free spectral functions for vectar mesons,
		=1 drop. mass, =2 broadening, =3 drop.+broad.
0,	IHARD:	=1 with charm and bottom; =0 - without
0,	IBweight_MC:	=0 constant step in B =DBIMP;
		=1 choose B by Monte-Carlo ISUBS times
		in interval [Bmin,Bmax]
0,	INUCLEI:	=1 reactions with kinetic deuterons
0,	**IPHQMD:**	=1: propagation with QMD dynamics;
		=0 with HSD/PHSD dynamics
		(flags below are used for IPHQMD=1 only)
0,	iqmdeos:	EoS for QMD mode :
		=0: hard static EOS;
		=1 soft static EoS;
		=2 soft EoS with mom. dep.endence
0,	ISACA:	enable or disable SACA output
		(note: SACA or MST is controlled by iflagsaca)
10.0,	TSACA:	starting time for SACA
5.0,	DTSACA:	time step for SACA calculations
25,	NTSACA:	Number of SACA timesteps
		(tmax=tsaca+dtsaca·ntsaca must be < FINALT)
0,	iflagsaca:	=1 SACA (and MST), =0 MST only, no SACA

MASSTA - mass of target nuclei
MSTAPR - number of protons in target nuclei
MASSPR - mass of projectile nuclei
MSPRPR - number of protons in projectile nuclei

Tkin - bombarding **'kinetic'** energy per nucleon in AGeV in laboratory frame (fixed target)
Center of mass energy: $s_{NN} = 2m_N(\text{Tkin} + 2m_N)$ with $m_N = 0.938$ GeV.

AGS: $^{197}_{79}$Au

Tkin	$\sqrt{s_{NN}}$	NUM
2	2.70	300
4	3.32	300
6	3.84	300
8	4.30	300
10.7	4.86	300

SPS: $^{208}_{82}$Pb

Tkin	$\sqrt{s_{NN}}$	NUM
19.062	6.27	300
29.062	7.62	300
39.062	8.76	300
79.062	12.32	300
157.062	17.27	200

RHIC: $^{197}_{79}$Au

Tkin	$\sqrt{s_{NN}}$	NUM
29.728	7.7	300
43.241	9.2	300
68.620	11.5	300
110.198	14.5	300
202.900	19.6	200
386.717	27	200
808.892	39	100
2 073.689	62.4	50
9 006.653	130	40
21 320.086	200	30

LHC: p + p

Tkin	$\sqrt{s_{NN}}$	NUM
13 433 047.164	5 020	150
26 119 401.109	7 000	150
90 085 285.970	13 000	100

LHC: $^{208}_{82}$Pb

Tkin	$\sqrt{s_{NN}}$	NUM
4 060 552.495	2 760	5
13 433 047.164	5 020	5

We note that even ELAB is requested in Lab frame, the calculations are done in the initial NN center-of mass frame for all type of reactions.

BMIN – minimal impact parameter b in fm
BMAX – maximal impact parameter b in fm
DBIMP – step in impact parameter b in fm (Δb). Used only if IBweight_MC=0
IBweight_MC – method to simulate impact parameter distribution from Bmin to Bmax. (cf. Chapter 2 for the details.)

1) **IBweight_MC=0**
The code runs from b_{min} to b_{max} with the step $db = DBIMP$. For the calculation of final cross sections one has to perform the integration over impact parameter b with the weight $(2\pi b)$ from b_{min} to b_{max}.
For example, the cross section for pion production in Au+Au collisions [in mb] in

some centrality class from b_{min} to b_{max} is defined as

$$\sigma_\pi = 10 \int_{b_{min}}^{b_{max}} db\ 2\pi\ b\ N_\pi(b) \Rightarrow 10 \sum_{b_{min}}^{b_{max}} \Delta b\ 2\pi\ b\ N_\pi(b). \tag{1.4.1}$$

Here the factor 10 is to transform the result from fm^2 to mb. The function $N_\pi(b)$ is the pion multiplicity for given impact parameter b.
The multiplicity of particle type i (e.g. $i = \pi$) for given impact parameter b is defined as the sum of all particles type i (N_i) divided by the 'weight' factor (NUM·ISUBS) which is the number of events for given b in all ISUBS runs:

$$N_i(b) = \sum_{j=1}^{N_i} \frac{1}{\text{NUM} \cdot \text{ISUBS}}\ . \tag{1.4.2}$$

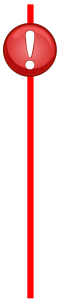

Note: even for p+p or p+d set DBIMP=1 (or some NON zero number!). This parameter is not used for p+p and p+d explicitly, however, enters in the organization of the main routine. The initialization for p+p is done by placing two protons in front of each other (i.e. b=0 fm). For the p+d collisions the deuteron target is initialized in momentum space using the Paris wave function with a high momentum tail – for the details see Ref. [38].

2) **IBweight_MC=1**
The impact parameter b is chosen by Monte-Carlo ISUBS times with the proper weight $P(b) = 2\pi b$ from b_{min} to b_{max}. In this case no extra weighting ($db\ 2\pi\ b$) is needed for the calculation of observables! E.g. the pion multiplicity in the centrality class from b_{min} to b_{max} is defined as

$$N_\pi = \sum_{j=1}^{N_i} \frac{1}{\text{NUM} \cdot \text{ISUBS}}\ , \tag{1.4.3}$$

where N_i is the number of pions in all simulated events in the interval $[b_{min}, b_{max}]$. The corresponding cross section for pion production in Au+Au collisions [in mb] in centrality class from b_{min} to b_{max} is defined as

$$\sigma_\pi = N_\pi \cdot \sigma_{geom}, \tag{1.4.4}$$

where $\sigma_{geom} = \int_{b_{min}}^{b_{max}} db\ 2\ \pi\ b = \pi\ b^2 \Big|_{b_{min}}^{b_{max}}$

NUM - number of parallel events in each subsequent run ISUBS.
The HSD code is based on the parallel ensemble method (contrary to e.g. UrQMD, which is an event by event generator). In this way one can simulate simultaneously many (NUM) nucleus-nucleus collision - 'events'. The interaction between the particles is allowed *only* inside one event. However, such parallel ensemble algorithm allows to compute collective quantities (baryon or meson densities, temperature etc.) at a given time with good accuracy since the statistical fluctuations are much

reduced by averaging over events. This is very important for the calculation of the hadron potentials (which depend on density etc.) as well as for the investigation of the in-medium properties of particles (since the spectral functions, self-energies also depend on density, temperature etc.).

Do not increase NUM too much! Remember - all produced particles are stored in vectors, so, if NUM is too big, there is no storage left and the code will stop with the messages: *'Too many test particles'* if the number of initial baryons is beyond the limit or *'Too many mesons'* if the number of produced particles is out of dimension. In this case decrease NUM and alternatively increase ISUBS. Some 'optimal' NUM (for orientation) are given in the previous page.

ISUBS - number of subsequent runs

In order to improve statistics one can run the code many (ISUBS) times, but collect the output information in the same files (which simplifies the analysis). Equivalently: use ISUBS=1, but submit the job many times and store the output files.

ISEED - any integer number to initialize of random number generator

IDILEPT - flag to activate perturbative dileptons:

IDILEPT=0 - without dileptons,
IDILEPT=1 - electron pairs (e^+e^-),
IDILEPT=2 - muon pairs ($\mu^+\mu^-$)

ICQ - flag to activate the in-medium effects for vector mesons:

ICQ=0 - without in-medium effects (free spectral functions),
ICQ=1 - dropping mass scenario,
ICQ=2 - collisional broadening,
ICQ=3 - dropping mass + collisional broadening

IHARD - flag to activate charm/bottom dynamics:

IHARD=0 - without charm/bottom degrees of freedom,
IHARD=1 - with charm/bottom degrees of freedom

FINALT - final time of calculation [fm/c]

Note: final calculation time t_{max}
The PHSD code is running with a dynamical time step up to the maximum time t_{max}. In order to simplify the initialization for the user we parametrized the time t_{max} as a function of the initial energy ($\sqrt{s}$):

$$t_{max} = 35 + \frac{170}{\sqrt{s}\ [\mathrm{GeV}]} [\mathrm{fm/c}] \tag{1.4.5}$$

This gives some 'optimal' computational time for the general tasks (particle multiplicities, spectra, rapidity distributions etc.) However, for some specific tasks (collective flow or some specific correlations) one needs to run the code longer (500 fm/c). Please, contact us for further explanations (or increase FINALT).

ILOW - output level (default=11)
INUCLEI - reactions with kinetic deuterons: = 1 yes, =0 no

IPHQMD - propagation of baryons with QMD dynamics:
=1 yes, =0 no, i.e. with HSD/PHSD dynamics

Note: flags below are used for IPHQMD=1 only !
iqmdeos - EoS for QMD mode :
=0: hard static EOS;
=1 soft static EoS;
=2 soft EoS with mom. dep.endence
ISACA - enable or disable SACA output
(note: SACA or MST is controlled by iflagsaca)
TSACA - starting time for SACA
DTSACA - time step for SACA calculations
NTSACA - Number of SACA timesteps
(tmax = tsaca + dtsaca·ntsaca must be < FINALT)
Note: total number of time steps for MST/SACA output is $NTSACA + 1$
iflagsaca =1 SACA (and MST), =0 MST only, no SACA

Note: p+A reactions
The proton initialization is done in form of a cylindrical beam profile perpendicular to the beam direction with transverse radius $R = R_T + 1$ fm, where R_T is the radius of the target nucleus. This implies that some 'distant' reactions will not show inelastic scattering. Such events can be excluded by (e.g.) looking at the final particles, e.g. the absence of newly produced particles indicates that this event is NOT inelastic. Also it is important to analyze the final events with respect to the experimental trigger conditions to obtain cross sections or multiplicities in accordance with the actual experimental setting.

Note: $\pi^- A$ reactions
The initialization of the pion beam in πA collisions is done in the Lab. frame in form of a cylindrical beam profile perpendicular to the beam direction with transverse radius $R = R_T + 1$ fm, where R_T is the radius of the target nucleus. This implies that some 'distant' reactions will not show inelastic scattering. Such events can be excluded by (e.g.) looking at the final particles: e.g. the absence of newly produced particles indicates that this event is NOT inelastic. Such events have to be excluded when calculating the total inelastic πA reaction cross section.

MASSPR and MSPRPR has to be set to zero for a pion beam! The parameters BMIN, BMAX, DBINP are NOT used for pion induced reactions. The initialization for $\pi - p$ is done by placing pion and proton in front of each other (i.e. b=0 fm).

1.5 General output files

The parameter for the output level (how much information is written out) is called `ILOW`, which provides the basic outputs:

- *phsd.dat* for all particles on event-by event basis using OSCAR format (for `ILOW = 10, 11, 12`),
- *FinaloutROOT* similar output in ROOT format (for `ILOW = 12`),
- *fort.888* for general output and parameter settings,
- *fort.80* for complementary information and errors (for control purpose only)
- *fort.300* separately for baryons from all events from all NUM (optionally - if `ILOW = 10`),
- *fort.301* separately for mesons from all events from all NUM (optionally - if `ILOW = 10`)

The default value is `ILOW = 12`. If `ILOW < 12`, for example 11, the ROOT output file is empty.
Note for ROOT output: In the makefile there is a check for ROOT availability. Only in that case the ROOT output file `FinaloutROOT()` (in finaloutROOT.f file) will be generated.

Please keep the information files about the collision, i.e. *inputPHSD* file and the parameter settings (*fort.888*) to know exactly which parameters were used in the simulation.

When one uses `ILOW < 10`, there are more files written outfor more information. The main outputs *fort.888* and *fort.80* are written by a lot of different routines including the main routine. The output files for final particles *fort.300* and *fort.301* are written out by the routine `FINALOUT300()` (in *finaloutPHSD.f*).

The 'output' is written *after the decays* of all baryonic ($\Delta, N(1535), N(1440), \Sigma^*$) and mesonic ($\rho, \omega, \phi, a_1, \eta'$, all K^*) resonances, however, *before the weak decays* of strange particles (Λ and Σ). The momenta of final particles are given in the *nucleon-nucleon center-of-mass frame in GeV/c*.

1.5.1 Optional output - *fort.300, fort.301* for ILOW=10

Output file *fort.300* - final baryons

ID(j,1)	ID(j,2)	ISUB	IRUN	P_X	P_Y	P_Z	P_0	b
...	...	...	...	...	...	...	...	...

Output file *fort.301* - final mesons

IPI(j,1)	IPI(j,2)	ISUB	IRUN	P_X	P_Y	P_Z	P_0	b
...	...	...	...	...	...	...	...	...

- ID(j,1) or IPI(j,1) is the type of particle j (cf. Tables 1, 2)
- ID(j,2) or IPI(j,2) is the electric charge
- ISUB is the number of subsequent run, changes from 1 to ISUBS (maximum, defined in *inputPHSD* file)
- IRUN is the number of current event, changes from 1 to NUM (maximum, defined in *inputPHSD* file)
- P_X, P_Y, P_Z, P_0 are the 3-momentum and energy of particle j in the nucleon center-of-mass frame
- b is the current impact parameter in fm; it changes from b_{min} to b_{max} (defined in *inputPHSD* file).

1.5.2 Event-by-events output - *phsd.dat*

This output collects baryons, mesons and photons in one single file *phsd.dat*. It is convenient for event-by-event analysis and for MC simulations of detectors. Each stored event consists of a header (2 lines) and particle list (number of lines defined in the header).

The extended output in *phsd.dat* with freeze-out coordinates and momenta of baryons can be written for `IFreezeOut=1`.

Output file *phsd.dat* - all particles - default - if `IFemto`=0

N	ISUB	IRUN	b	IBweight	ipdgTA	ipdgPR	SRTIN	Ratqgp
N_P	$\psi(2)$	$\varepsilon(2)$	$\psi(3)$	$\varepsilon(3)$	$\psi(4)$	$\varepsilon(4)$	$\psi(5)$	$\varepsilon(5)$
ID	Q	P_x	P_y	P_z	P_0	ID(J,5)/IPI(5,J)	ID(J,3)/IPI(3,J)	J
...	...	...	...	...	...	...	...	...

Output file *phsd.dat* - all particles - optional if `IFemto`=1

N	ISUB	IRUN	b	IBweight	ipdgTA	ipdgPR	SRTIN	Ratqgp	
N_P	$\psi(2)$	$\varepsilon(2)$	$\psi(3)$	$\varepsilon(3)$	$\psi(4)$	$\varepsilon(4)$	$\psi(5)$	$\varepsilon(5)$	
ID	Q	P_x	P_y	P_z	P_0	ID(J,5)/IPI(5,J)	ID(J,3)/IPI(3,J)	J	FZ
...	...	...	...	...	...	...		...	
where FZ = t_{last}	ρ_B	E_{loc}	$[X$	Y	Z	$t]$	$[P_X^f$	P_Y^f	P_Z^f	$P_0^f]$	ρ_B^f	E_{loc}^f

For the **header**:

- N is the number of particles in the event;
- `ISUB` is the current subsequent run;
- `IRUN` is the current parallel event;
- b is the current impact parameter in fm;
- `IBweight` = IBweight_MC:

  =0 impact parameter was selected from BMIN up-to BMAX with constant step DBIMP,

=1 from BMIN up-to BMAX by MC;

- `ipdgTA` is the pdg of TARGET;
- `ipdgPR` is the pdg of PROJECTILE;
- `SRTIN` is the invariant energy per NN in GeV;
- `Ratqgp` is the total ratio of energy from the QGP phase to the total energy in the current parallel event in fm/c;
- N_P is number of participants;
- $\psi(n)$ and $\varepsilon(n)$ are respectively the participant plane angle and eccentricity of the n^{th} harmonic:

$$\psi_n\{part\} = \frac{1}{n}\text{Atan}\,\frac{\langle r^n\ \sin(n\,\phi)\rangle}{\langle r^n\ \cos(n\,\phi)\rangle}$$

$$\varepsilon(n) = \frac{\sqrt{\langle r^n\ \cos(n\,\phi)\rangle^2 + \langle r^n\ \sin(n\,\phi)\rangle^2}}{\langle r^n\rangle}$$

where $r = \sqrt{(x-\overline{x})^2 + (y-\overline{y})^2}$ and $\phi = \text{Atan}\,(y-\overline{y})/(x-\overline{x})$ are the position and azimuthal angle of each participant from the center $(\overline{x}, \overline{y})$ of fireball.

For the **particle list**:

- ID is type of particle in PDG notation (cf. Tables 1.1 - 1.8),
- Q is electric charge,
- P_X, P_Y, P_Z, P_0 are the 3-momentum and energy of particle,
- `ID(J,5)`/`IPI(5,J)` is history of particle creation,
- ID(J,3) is information about parents ("J") for the final baryon coming from baryon resonance decay,
- J is position of the baryons in the PHSD ID vector

Extra output for `IFemto`=1: freeze-out information at last interaction:

- t_{last} = `baryonFZ(J)%RFZL(4)` - last interaction time (chemical +kinetic)
- ρ_B = `baryonFZ(J)%densBFZL` - baryon density at the last interaction time
- E_{loc} = `,baryonFZ(J)%EloccFZL` - energy density at the last interaction time
- $[X, Y, Z, T]$ = `baryonFZ(J)%RFZL(1:4)` - 3-coordinates and time of freeze-out.
- $[P_X^f, P_Y^f, P_Z^f, P_0^f]$ = `baryonFZ(J)%PFZL(1:4)` - last interaction : 3-momenta and energy
- ρ_B^f = `baryonFZ(J)%densBFZC` - chemical freeze-out : baryon density
- E_{loc}^f= `baryonFZ(J)%EloccFZC` - chemical freeze-out : energy density

1.5.3 Analysis programs to compute hadron spectra and v_n flow

The analysis programs in FORTRAN are stored in the PHSD-PHQMD subdirectory */ANALYSIS/FORTRAN*.
There we provide an example of the analysis routine - file `Analys-spectra-PHSD-PHQMD.f` -

which shows how to calculate general observables such as multiplicities, rapidity distributions and p_T spectra for hadrons (p, π, K etc.) from each A+A event individually as well as averaged over all events in selected centrality using *phsd.dat*.
Moreover, program `vn_flow_PHSD-PHQMD.f` provides an example how to compute v_n collective flow on event-by-event basis using *phsd.dat*.
The programs require *inputPHSD* file and *phsd.dat* and show an example how to combine the results simulated in different subdirectories to gain statistics.

1.6 Cluster production in PHQMD mode

In the PHSD–PHQMD framework, the propagation of mesons and partons follows the PHSD approach, while baryons evolve according to QMD dynamics.

Clusters can be identified using two methods:
1) `MST` -the minimum spanning tree procedure or
2) `SACA` - a cluster-finding algorithm based on simulated annealing, known as the simulated annealing clusterization algorithm.

The MST algorithm relies on spatial correlations and is effective for identifying clusters at the late stage of the reaction. To identify clusters at earlier times—when nucleon–nucleon collisions are still ongoing and the nuclear density remains high—the SACA approach is employed. For collision energies relevant to RHIC BES-II, CBM, HIAF, and NICA, the MST method is generally sufficient, whereas for very low-energy collisions (on the order of MeV), SACA is more appropriate. We emphasize that both MST and SACA are cluster recognition procedures rather than "cluster formation" mechanisms, since PHQMD propagates baryons, not preformed clusters.

However, the MST approach identifies only geometrical clusters and does not account for momentum-space correlations or binding energies. To address this, an advanced minimum spanning tree (aMST), sometimes referred to as a stabilization procedure, is introduced. This method retains only clusters with negative binding energy and allows for the recombination of nucleons that have left a cluster without undergoing rescattering, thereby improving the physical consistency of the identified clusters.
3) Additionally, the `kinetic mechanism for deuteron production` is incorporated by catalytic hadronic reactions accounting for all isospin channels of the various $\pi NN \leftrightarrow \pi d$, $NNN \leftrightarrow Nd$ reactions.

1.6.1 Output for kinetic deuterons in file 'phsd.dat'

Kinetic mechanism: Deuterons can be created in catalytic hadronic reactions as $\pi NN \leftrightarrow \pi d$ and $NNN \leftrightarrow Nd$ in different isospin channels. The quantum nature of the deuteron is considered through an excluded volume, which forbids its production if another hadron is localized in this volume, i.e. a deuteron with a rms radius of about $\sqrt{< r_d^2 >} \simeq 2.1$ fm cannot be formed if between the p and the n other hadrons are located. We project furthermore the relative momentum of the incoming nucleons onto the deuteron wave function in momentum space. These quantum corrections lead to a significant reduction of deuteron production by the kinetic mechanism, particularly at target/projectile rapidities.

We note that the kinetic deuterons are propagated explicitly in the PHQMD as a degree-of-freedom (contrary to the nucleons in MST clusters, which are propagated as nucleons. We refer the reader to Ref. [5] for the details.

The kinetic deuterons are produced in PHQMD and PHSD modes if flag `INUCLEI`=1 in *inputPHSD*. They are written in phsd.dat file.

Note: in *phsd.dat* the deuteron has ID number "100121", however the PDG number is "1000010020" according to the PDG naming rule for clusters:
±10LZZZAAAI, where Z - number of protons, AA – mass number (total nucleons), L –

Table 1.9: The **Deuteron** identification codes. Kinetic deuterons

ID(j,1)	ID(j,2)	type	ID(PDG-type)	mass* [GeV]
101	1	d	100121	1.8756

number of strange quarks (usually 0 for normal nuclei), I – isomer state (0 for ground state).

1.6.2 Output for clusters identified by MST/SACA

The PHQMD model has two algorithm for cluster identifications:

- **MST** (Minimum Spanning Tree)
- **SACA** (Simulated Annealing Clusterization Algorithm)

The mode is selected via

$$iflagsaca = \begin{cases} 0 & \text{MST} \\ 1 & \text{SACA} \end{cases} \tag{1.6.1}$$

which is defined in *inputPHSD* file.

MST clusters: The attractive potential between baryons with a small relative momentum keeps them close together and can lead to a group of bound nucleons. Such groups of co-moving nucleons can be identified as clusters during the dynamical evolution, using the advanced Minimum Spanning Tree (aMST) method, as detailed in Ref. [5]. MST [26] collects nucleons, which are close in coordinate space. At a given time t a snapshot of the positions and momenta of all nucleons is recorded and the MST clusterization algorithm is applied: two nucleons i and j are considered as "bound" to a deuteron or to a larger cluster $A > 2$ if they fulfill the condition

$$|\mathbf{r}_i^* - \mathbf{r}_j^*| < r_{clus}\,, \tag{1.6.2}$$

where on the left hand side the positions are boosted in the center-of-mass of the ij pair. The maximal distance between cluster nucleons, $r_{clus} = 4$ fm, corresponds roughly to the range of the attractive NN potential. Additionally, in aMST the clusters have to be bound ($E_B > 0$).

aMST corrects only the fact that in semiclassical systems a nucleon can acquire more kinetic energy than in the corresponding quantum system because all other nucleons can have negligible momenta what is not the case in the quantum system. This leads to an enhanced emission of nucleons from semiclassical clusters, which has to be corrected. It is important to highlight that MST serves as a tool for cluster recognition at each time step by determining the nucleons, which form a cluster under the above conditions. It is not a mechanism for 'building' clusters, which are then propagated, since the QMD transport model propagates baryons and not clusters. At the end of the heavy ion reaction the

clusters as well as the nucleons, which are part of a cluster, do not change anymore. This allows to determine the asymptotic cluster observables.

SACA clusters: The clusters are identified by the MST (Minimum Spanning Tree) or the SACA ('Simulated Annealing Cluster Algorithm') algorithm which finds the most bound configuration of nucleons and clusters [4].

The MST/SACA clustering routine provides detailed information on clusters and baryons identified by the MST/SACA clustering algorithms at selected time steps according to the setup in *inputPHSD* :

$$tmax = tsaca + dtsaca \cdot ntsaca \text{ (must be } < \text{FINALT)}$$

1.6.3 Cluster Output files

The cluster information obtained with the MST/SACA is stored in the files:
`fort.790` (MST), `fort.792` (SACA)
The corresponding anti-cluster information is written to
`fort.780`, `fort.782`

Only baryons that are active in the clustering procedure are written to these output files. Thus, only fully formed baryons are considered; baryonic resonances, baryons still within their formation time, and leading baryons are excluded. Currently, cluster formation in the MST/SACA includes neutrons (n), protons (p) and hyperons (Λ, Σ^0).

List of output files for clusters:

File	Content
fort.790	clusters + free baryons (MST)
fort.792	clusters + free baryons (SACA)
fort.780	anti-clusters + free anti-baryons (MST)
fort.782	anti-clusters + free anti-baryons (SACA)
fort.791	all baryons entering MST clustering
fort.793	all baryons entering SACA clustering
fort.781	antibaryons entering MST clustering
fort.783	antibaryons entering SACA clustering
fort.770	kinetic deuterons (written in `FRIGA_QMD.f`)

Output *header* for each cluster : `nclusterSM`, `iMST`, LSIZE_POT2, rcluster :

- `nclustersm` = total number of single (p, n, Λ) and clusters
- `iMSTSACA` 1 for MST , 2 for SACA
- LSIZE_POT2 - internal number of clusters in the cluster vector for MST/SACA
- `rcluster` = MST cluster radius

Column	Description
1	cluster number in recording vector $[1, \ldots, N_{\text{cluster}}]$
2	cluster charge $Z_{\text{cluster}} = Z_p N_p$
3	number of neutral neutral baryons in cluster $N_B = N_n + N_\Lambda + N_{\Sigma^0}$
4–6	average baryon momentum in cluster $\langle p_i \rangle = P_{\text{cluster}}/A_{\text{cluster}}$ [GeV/c]
7–9	cluster center-of-mass position in A+A frame (X, Y, Z) [fm]
10	cluster rapidity in the $A + A$ frame
11	average baryon mass in cluster $\langle m_i \rangle = M_{\text{cluster}}/A_{\text{cluster}}$ [GeV]
12	cluster mass $M_{\text{cluster}} = \sum_i m_i$ [GeV]
13	number of Λ hyperons in cluster
14	number of Σ^0 hyperons in cluster
15	binding energy per baryon $E_{\text{bin}} = E_{\text{bin}}^{\text{cluster}}/A_{\text{cluster}}$ [GeV]

FORTRAN output format:

```
format(1x,3I4,9(1XE11.4),2(1XI4),3(XE10.3),12(XE10.3))
```

1.6.4 Baryon Output from clustarization routines

Besides the identified clusters, the output also contains all nucleons and hyperons (and antibaryons) entering the clustering procedure, including both cluster-bound baryons and free baryons not assigned to any cluster.

Baryon ID_{QMD} convention according to QMD "iso" vector, used only for output for clusters:

ID_{QMD}	Particle
0	neutron (n)
1	proton (p)
17	Λ
18	Σ^0

Files: baryons `fort.791` (MST), `fort.793` (SACA) Anti-baryons: `fort.781`, `fort.783`

Column	Description
1	baryon index $[1, \ldots, N_{\text{particles}}]$
2	baryon ID_{QMD} from QMD "iso" vector (see table above)
3–5	baryon momentum (P_x, P_y, P_z) [GeV/c]
6–8	baryon position (X, Y, Z) [fm]
9	baryon mass [GeV]
10	cluster number to which baryon belongs
11	cluster size A_{cluster} to which this baryon belongs
12	original position "J" of baryon in the PHSD vector (integer number)
13	MST: same as column 10; SACA: MST precalculation cluster index
14	MST: same as column 11; SACA: MST precalculation cluster size
15	PHQMD: $ID(J, 6)$ (projectile/target origin or collision)
16	PHQMD: $ID(J, 5)$ production channel
17	last interaction time T_{last} [fm/c]
18	cluster binding energy per baryon [GeV]

FORTRAN output format:

```
format(1x,2I4,7(1XE11.4),2(1XI3),3(1XI10),2(1XI10),(1XE11.4))
```

The history of baryons inside clusters can be reconstructed using the files baryons from MST `fort.791` and antibaryons from MST `fort.781` or baryons from SACA `fort.793` and antibaryons from SACA `fort.783`.

Firstly these files converted to `fort.8XX` files by applying aMST routine for stabilization procedure *781to891.f*.

Matching the original PHSD index J (column 12) together with the last interaction time T_{last} (column 17) allows synchronization with the `phsd.dat` event record and the study of cluster stability.

1.6.5 FORTRAN conversion into dat-file

The analysis routine `analys-clusters-PHQMD.f` (written in FORTRAN) is located in subdirectory `/ANALYSIS/Analysis_cluster/`

1. The purpose of the code:
The code takes as input the cluster files (e.g., fort.791, fort.781) obtained from the MST approach and performs a stabilization procedure using the aMST method. The resulting cluster information is subsequently combined with particle data from phsd.dat to generate a new output file, phqmd.dat. This implementation is written in Fortran. A corresponding C++ version for ROOT users is also available.

2. Input files:
inputPHSD (initial setup);
fort.791 (all baryons entering MST clustering);
fort.781 (all anti-baryons entering MST clustering);
phsd.dat (all particles including mesons and bayons).

3. Output files:
phqmd.dat (output the all particles (same as phsd.dat), but include cluster labels.);
fort.892 (all baryons entering aMST clustering. If iOUT892=1, enables output, while iOUT892 = 0 disables it.);
fort.882 (all anti-baryons entering aMST clustering. If iOUT882=1, enables output, while iOUT882 = 0 disables it.).

The header of the phqmd.dat is identical to that of the phsd.dat. FORTRAN output format of the particle list in phqmd.dat:
format(1X,1I8,1I6,4E16.8,3X,I6,2X,I8,2X,I10,2X,I10,2X,I10,2X,1E11.4,2X,1E11.4)
The meaning of each column (1-9 columns are the same as phsd.dat):

Column	Description
1	ID type of particle in PDG notation
2	electric charge Q
3–5	three momentum (P_x, P_y, P_z) [GeV/c] of particle
6	energy of particle [GeV]
7	ID(J,5)/IPI(5,J). The history of particle creation
8	ID(J,3). Information about parents ("J") for the final baryon
9	J. The position of the baryon in the PHSD ID vector
10	cluster number to which baryon belongs
11	cluster size A_{cluster} to which this baryon belongs
12	last interaction time T_{last} [fm/c]
13	cluster binding energy per baryon [GeV]

The format and the meaning of each column in fort.892 (fort.882) are the same as those in fort.791 (fort.781).

5. Get clusters from the phqmd.dat:

With the information provided in columns 10 and 11, one can perform a cluster analysis to identify possible clusters. For example, if column 10 assigns a cluster ID of 1 and column 11 indicates a cluster size of $A = 5$, this implies that there are four additional baryons belonging to the same cluster. The total binding energy of the cluster is given by the sum of the values listed in column 13.

We emphasize that the identified clusters are not necessarily "real" clusters, in the sense of experimentally established clusters so far. The user may choose whether to retain these clusters or not. If not, the constituent particles can instead be treated as free baryons.

For mesons, columns 10, 11, 12, and 13 are set to 0.

6. How to run `analys-clusters-PHQMD.f`

1. **Check the input files**
   Ensure that all required input files (`inputPHSD`, `fort.791`, `fort.781`, and `phsd.dat`) are located in the same folder. Usually, there are multiple folders corresponding to different jobs, for example `job-1`, `job-2`, etc.
2. **Compilation**

   ```
   ifort/gfortran -o analys-clusters-PHQMD.exe analys-clusters-PHQMD.f
   ```

3. **Place the executable** Copy the executable file `analys-clusters-PHQMD.exe` into the same directory as the corresponding `job-n` folder. This location can also be modified directly in `analys-clusters-PHQMD.f`.
4. **Run the program**

   ```
   ./analys-clusters-PHQMD.exe
   ```

5. **Provide the required input**
   During execution, the program will ask for the number of jobs and for the location of the corresponding `job-n` folders. These folders may be located either in the current working directory or in a subdirectory.
6. **Output files**
   The output files are written to the same folders that contain the input files.

1.6.6 ROOT Converter into UniGen format

The root-conversion macro converts the PHSD-PHQMD output files into a root-file in UniGen format containing full events with hadrons & clusters.

This code is located in subdirectory `/ANALYSIS/Analysis_cluster/root_unigen`
File `Readme.md` includes the detailed instruction how to run the converter.

The conversion merges the hadron output file `phsd.dat` with the cluster file `fort.891` and, optionally, the anti-cluster file `fort.881` for the last timestep. In the UniGen-file, hadrons and clusters are stored as particles with `GetWeight() = 1`, while cluster baryons are additionally stored as single baryons with `GetWeight() = 0`.

Required input files

- `inputPHSD`
- `phsd.dat`
- `fort.891`
- `fort.881` (optional, for anti-clusters)

Output files

- `phqmd.root`
- `phqmd_freeze.root` (optional, in freeze-out mode)

Available macros

- `convert_phqmd_detector_unigen.C`: standard PHQMD output
- `convert_phqmd_detector_unigen_freezeout.C`: output with `IFreezeOut=1`

Requirements The conversion requires ROOT (preferably with C++17 support) and UniGen. The UniGen library path must be adjusted in `macro/rootlogon.C` so that the appropriate shared library is loaded.

Running the conversion For standard PHQMD output without freeze-out coordinates:

```
root -l convert_phqmd_detector_unigen.C
```

For PHQMD output with freeze-out coordinates:

```
root -l convert_phqmd_detector_unigen_freezeout.C
```

The output is written to

`indir/unigen/smallclusters`

or

`indir/unigen/allclusters`

depending on the selected conversion options. These directories must exist before running the macro.

Main settings The standard conversion macro is called with

```
convert_phqmd_detector_unigen.C(
  TString indir,
  TString dataset,
  Int_t firstevent,
  Bool_t ConvertMode,
  Bool_t ConvertAnti)
```

where `indir` is the input directory, `dataset` is a unique output folder name, and `firstevent` allows continuous event numbering across several runs.

The option `ConvertMode` controls how clusters are treated. In mode 0, clusters are identified according to `cluster_table.dat`. In mode 1, stable small clusters are identified through the cluster table, while clusters with mass number $A > 7$ are counted independently of their physical existence. Baryons from unphysical clusters are written as single baryons.

The option `ConvertAnti` switches the conversion of anti-clusters on or off. This is useful because PHQMD stores clusters and anti-clusters in separate files.

Freeze-out mode For runs with `IFreezeOut=1`, the corresponding macro provides two additional switches:

- `WriteUnigen`: writes the UniGen file with freeze-out positions (but no freeze-out momenta)
- `WriteEventFreeze`: writes a ROOT file including freeze-out momenta

The latter can be read with `read_events_freeze.root`.

Additional remarks The file `cluster_table.dat` defines the physically allowed clusters, including their baryon content and branching ratios, and can be adapted if needed. Deuterons may originate either from the MST algorithm or from kinetic interactions; this information is stored in the particle status field. For other PHQMD cluster finding modes than aMST, the cluster input files must be replaced accordingly, e.g. `fort.893`/`fort.883` for SACA mode.

Chapter 2

Initial conditions

2.1 Centrality selection by impact parameters

The PHSD–PHQMD code is based on the **parallel ensemble method**, i.e. the simultaneous simulation of many (NUM) events. This approach is essential for the calculation of mean–field quantities such as the baryon density, scalar density, and local energy density. These quantities play a crucial role in the dynamical evolution of the system, as they enter the evaluation of hadronic mean-field potentials and the in-medium properties of particles (both hadrons and partons).

For a given impact parameter b, a number of NUM parallel ensembles (specified in the *inputPHSD* file) are initialized. Each ensemble follows an independent Monte-Carlo chain; therefore, the ensembles can be interpreted as NUM statistically independent events simulated at the same impact parameter b.

In this sense, NUM effectively provides an additional statistical dimension in the distribution $P(b, \mathrm{NUM})$, corresponding to different realizations of the same collision configuration. This concept is illustrated in Figs. 2.1 and 2.2.

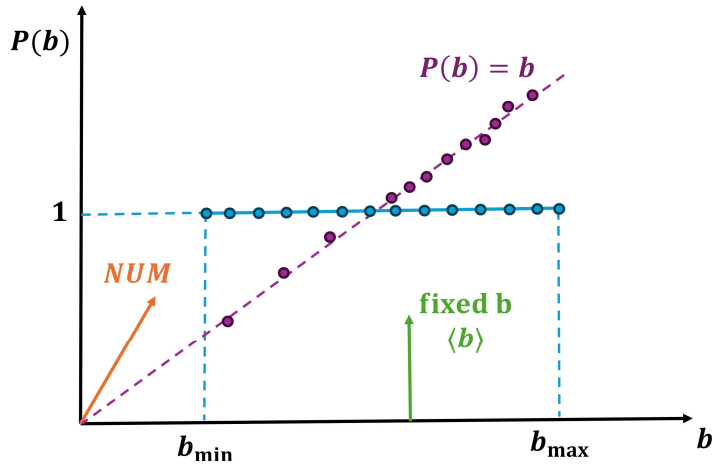

FIG. 2.1: Probability distribution $P(b)$ as a function of the impact parameter b in PHSD-PHQMD. One can use a fixed impact parameter, or a range (b_{min}, b_{max}), or the minimum bias distribution (see text for explanations).

For the initial impact parameter, the PHSD-PHQMD has two possibilities which are

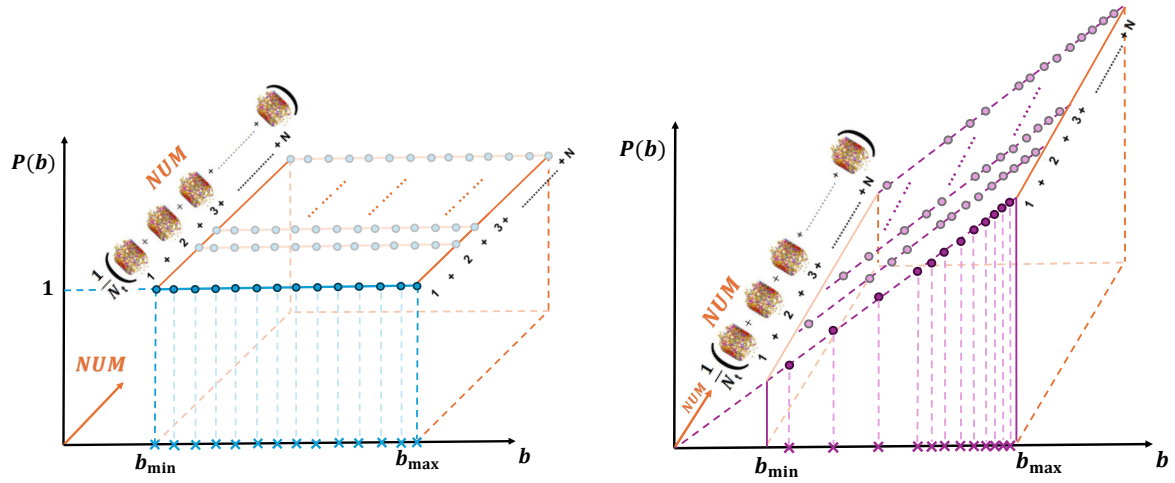

FIG. 2.2: Probability distribution $P(b)$ for NUM "events", i.e. parallel ensembles (see text for explanations).

controlled by `IBweightMC` parameter set in *inputPHSD*.

1.) `IBweightMC=1` :
For the minimum bias possibility, one can play with the distribution function using `IBweightMC=1` (set in *inputPHSD*). The minimum bias distribution is:

$$P(b) = \frac{2\pi\ b\ db}{\int_{b_{min}}^{b_{max}} 2\pi\ b\ db}, \tag{2.1.1}$$

In this case, the impact parameter would be chosen by Monte Carlo in the range (b_{min}, b_{max}) with the Min. Bias probability.

2.) `IBweightMC=0` :
One can also perform the calculation for a range (b_{min}, b_{max}) with a step DBIMP, with a constant probability (`IBweightMC=0`), or for a fixed value of the impact parameter, which would be the mean value of the Minimum Bias distribution on the range (b_{min}, b_{max}) : $\langle b \rangle_{Min.Bias} = \int_{b_{min}}^{b_{max}} b\ P(b)$

When you use `IBweightMC=1` it means that the impact parameter b is chosen randomly (according to the Min.Bias probability $P(b)$), however, for each selected b there will be `NUM` events simulated. The number of selected b correspond to `ISUBS` from *inputPHSD*. Thus, when you set `ISUBS=20`, it means that you have **only** 20 values of impact parameter b. It is by example too small sampling for flow evaluation, in this case it is recommended to perform the calculation for a range (b_{min}, b_{max}) with a step DBIMP, and then weight the results with the Min. Bias probability.
Moreover, if you want to have all this NUM events at the same initial conditions (i.e. eccentricity), better to chose `ISINGLE=1` (in *ini_param.f*).

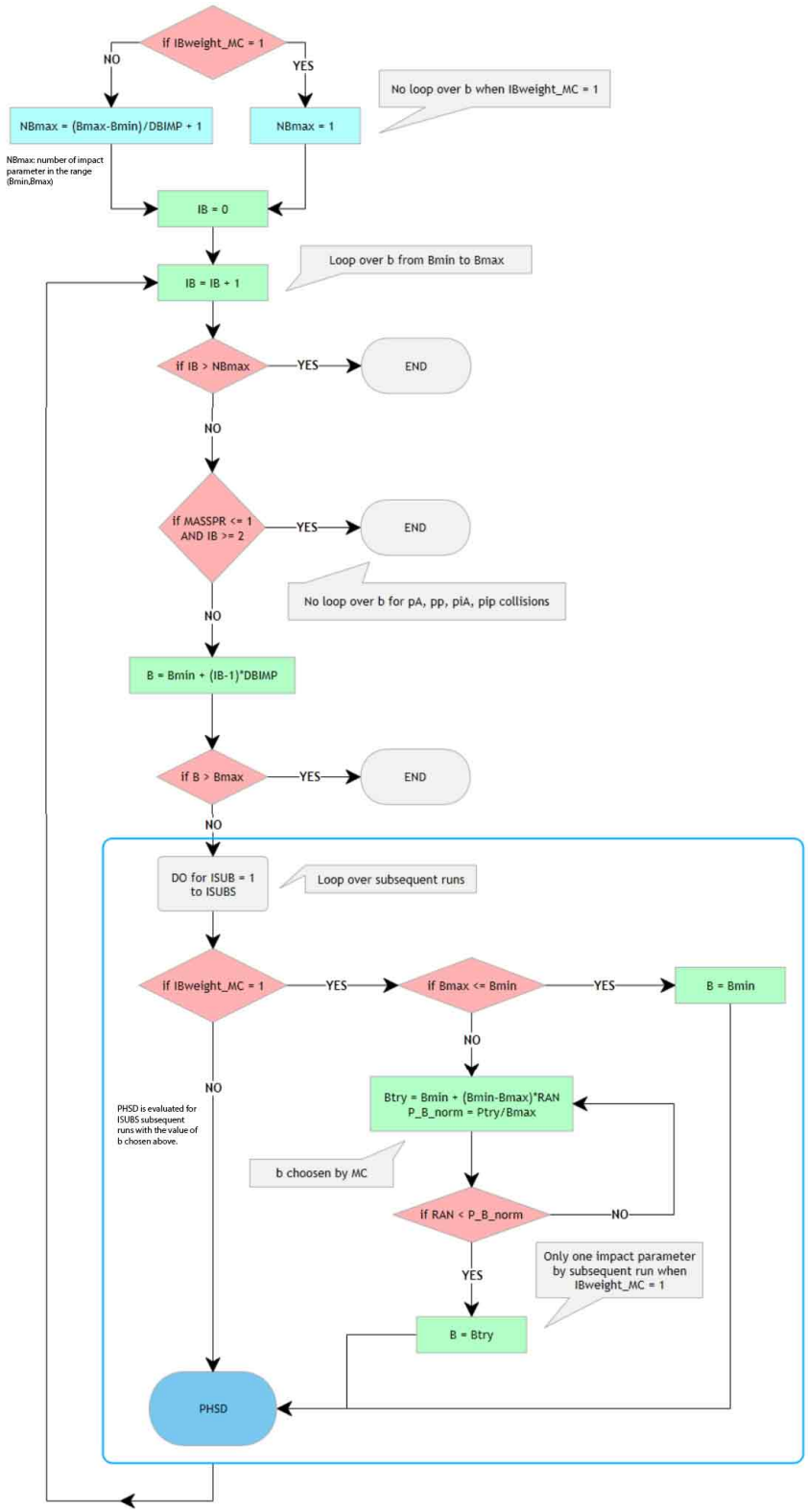

FIG. 2.3: Algorithm showing the two different options for the choice in impact parameter. For `IBweightMC=1` the impact parameter is chosen by Monte Carlo according to the Min. Bias probability. For `IBweightMC=0` it is simply chosen with a constant probability from a range (b_{min}, b_{max}) with a step DBIMP.

The total cross section of a reaction for a given range of impact parameter is :

$$\sigma_{tot} = \sum_{i=b_{min}}^{b_{max}} \sum_{j=events} N_i^j \times \sigma_{geom}, \tag{2.1.2}$$

with

$$\sigma_{geom} = \pi(b_{max}^2 - b_{min}^2). \tag{2.1.3}$$

For example for a fixed impact parameter b, one use many parallel events `NUM`, and/or subsequent runs `ISUB`. For each event, we initialize the system in coordinate and momentum space [39].

2.2 Initialization of a nucleus

The initial nucleon density for a heavy nucleus is usually parameterized by a Fermi distribution with three parameters, known as the Wood-Saxon distribution:

$$\rho(r) = \rho_0 \frac{1 + \omega(r/R)^2}{1 + \exp\left(\frac{r-R}{a}\right)}, \tag{2.2.1}$$

where ρ_0 corresponds to the nucleon density in the center of the nucleus, $R = R_0 A^{1/3}$ corresponds to the nuclear radius (with A the atomic number and $R_0 = 1.096$ fm (in PHSD) being the volume occupancy of a nucleon), a to the skin depth, and ω characterizes deviations from a spherical shape.

Such for ^{197}Au ($R = 6.38$ fm, $a = 0.535$ fm, $\omega = 0$) and ^{63}Cu ($R = 4.20641$ fm, $a = 0.577$ fm, $\omega = 0$), the nuclei so far employed at RHIC, $\rho(r)/\rho_0$ is shown in Figure 2.4 (left).

For a light nucleus a shell model distribution is used which is shown in the middle part of Figure 2.4 for Be, B, C, N and O as a function of the radius (cf. Book: L. R. B. Elton, Nuclear sizes, Clarendon Press, Oxford University Press, London, 1961. 114p. 15s.)

The distribution of the proton-neutron distance in the deuteron as given by the Hulthén wave function (from Ref. [39]) - right part of Figure 2.4.

In the Monte Carlo procedure, the radius of a nucleon is drawn randomly from the distribution $4\pi r^2 \rho(r)$ (where the absolute normalization is of course irrelevant).

We note that the PHSD has an option to initialize the uranium U target in coordinate space depending on special orientation.

In momentum space, the initial energy for each nucleon is determined using Fermi motion

$$p_F = \hbar c \left(\frac{3}{2}\pi^2 \rho\right)^{1/3}, \tag{2.2.2}$$

with $\rho = \rho(r)$ given by the Wood-Saxon distribution in space. The initial momentum is given by Monte-Carlo as $0 < p < p_F$.

For the details of the initialization in the `PHQMD mode` we refer to Ref. [4]. We note that the potential interaction is accounted during the initialization in both PHSD and PHQMD modes.

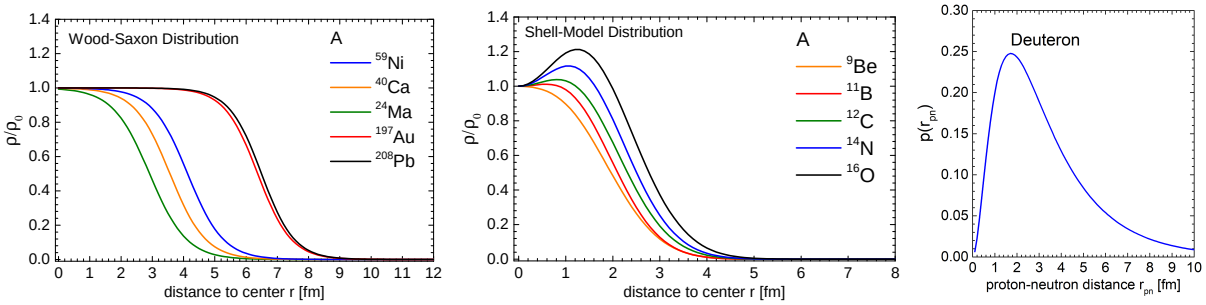

FIG. 2.4: Left: Woods-Saxon distribution as a function of the distance to the center of the nucleus r for Ni,Ca,Ma,Au and Pb. Middle: Shell model distribution as a function of the radius of the nucleus for Be,B,C,N and O. Right: Distribution of the proton-neutron distance in the deuteron as given by the Hulthén wave function (from Ref. [39]).

2.3 Box simulations

To study the properties of an infinite quark–gluon plasma (QGP) matter, as investigated in lattice QCD (lQCD) calculations, one can perform so-called "box simulations". In this case, the system is initialized in a finite box with periodic boundary conditions, effectively mimicking an infinite medium. After sufficient evolution time, the system approaches thermal and chemical equilibrium.

Box simulations are a standard tool in microscopic transport theory and are frequently used to verify the correct implementation of detailed balance in numerical models.

The simulation in a box [40] (from V. Ozvenchuk) are done using the routine `INIBOXPART` . This routine provides the initial conditions for 4-momentum and space position distribution of partonic test-particles in a box.

Chapter 3

Dynamics

3.1 Kadanoff-Baym off-shell dynamics in the PHSD

We stress that the PHSD [1, 2, 6, 7, 8, 3] is a microscopic covariant transport approach for the dynamical description of **strongly interacting hadronic and partonic matter** created in heavy-ion collisions. It is based on a solution of the Cassing-Juchem generalised off-shell transport equations for test particles [41, 42], which are derived from the Kadanoff-Baym equations [9] in first-order gradient expansion [10, 2] (cf. also the book [43]). This quantum field theoretical basis distinguishes the PHSD from the semi-classical BUU based model, since the PHSD propagates Green's functions (in phase-space representation) which contain information not only on the occupation probability (in terms of the phase-space distribution functions), but also on the properties of hadronic and partonic degrees-of-freedom via their spectral functions.

The PHSD approach consistently describes the full evolution of a relativistic heavy-ion collision from the initial hard scatterings and string formation through the dynamical deconfinement phase transition to the strongly-interacting quark-gluon plasma (sQGP) as well as hadronization and the subsequent interactions in the expanding hadronic phase as in the Hadron-String-Dynamics (HSD) transport approach [44, 45].

3.2 Quantum-Molecular Dynamics in the PHQMD

The QMD equation-of-motions (EoM) for a N-body system (i.e. system of N interacting nucleons) are derived using the Dirac-Frenkel-McLachlan approach [46, 47], which has been developed in chemical physics and later applied to nuclear physics for QMD like models [48, 26, 49, 29]. It is based on the variational principle for the Schrödinger equation, where the time evolution of the N-body wave function ψ is obtained from the variation

$$\delta \int_{t_1}^{t_2} dt < \psi(t)|i\frac{d}{dt} - H|\psi(t) >= 0, \tag{3.2.1}$$

where H is the N-body Hamiltonian. Eq. (3.2.1) can be formally solved by approximating the N-body wave function by the direct product of single particle "trial" wave functions (neglecting antisymmetrization) $\psi = \prod_i^N \psi_i$.

With the assumption that the wave functions have a Gaussian form and that the width of the wave function is time independent, one obtains two equations-of-motion for

the time evolution of the centroids of the Gaussian single particle Wigner density, which resemble the EoM of a classical particle with the phase space coordinates $\mathbf{r_{i0}}, \mathbf{p_{i0}}$ [26]:

$$\dot{r}_{i0} = \frac{\partial \langle H \rangle}{\partial p_{i0}} \qquad \dot{p}_{i0} = -\frac{\partial \langle H \rangle}{\partial r_{i0}} \quad . \tag{3.2.2}$$

We stress that the difference to the classical EoM is that here the expectation value of the quantal Hamiltonian is used and not a classical Hamiltonian. The Hamiltonian of the nucleus is the sum of the Hamiltonians of the nucleons, composed of kinetic and two-body potential energy, which has a strong interaction and a Coulomb part

$$H = \sum_i H_i = \sum_i (T_i + \sum_{j \neq i} V_{ij}). \tag{3.2.3}$$

The expectation value of the Hamiltonian, which enters Eq. 3.2.2 is finally given by

$$\begin{aligned} \langle H \rangle &= \langle T \rangle + \langle V \rangle & (3.2.4)\\ &= \sum_i \left(\sqrt{p_{i0}^2 + m^2} - m \right) & (3.2.5)\\ &+ \sum_i \langle V_{Skyrme}(\mathbf{r}_{i0}, t) + V_{mom}(\mathbf{r}_{i0}, \mathbf{p}_{i0} t) + V_{coul}(\mathbf{r}_{i0}, t) \rangle. \end{aligned}$$

In PHQMD the potentials used correspond to the hard, the soft and the soft momentum-dependent equations-of-states which are illustrated in Fig. 3.1 and the parameters for the three equations-of-state are presented in Table 3.1. Soft and soft momentum-dependent EoS have for cold nuclear matter the same $\frac{E}{A}(\rho)$.

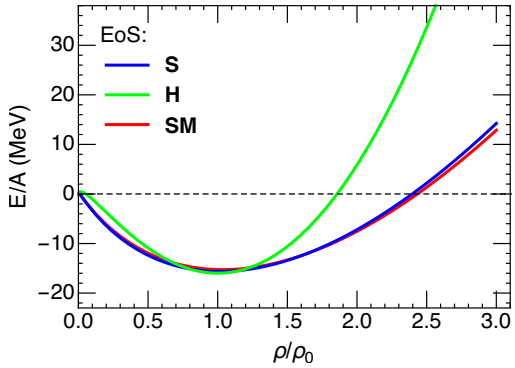

FIG. 3.1: Equation-of-state for $T = 0$ for the hard (green line), soft (blue line) and the soft momentum-dependent potential (red line).

In Ref. [25] is the momentum dependence of the two body interaction between two nucleons $V_{mom}(\mathbf{r}_{i0}$ has been implemented in the PHQMD additionally to the static Skyrme potential based on the Schrödinger equivalent potential obtained by averaging the two body potential $V(\mathbf{p}, \mathbf{p}_1)$ over the Fermi distribution of the cold target nucleons,

$$U_{opt}(p) = \frac{\int^{p_F} V(\mathbf{p}, \mathbf{p}_1) dp_1^3}{\frac{4}{3}\pi p_F^3}. \tag{3.2.6}$$

The experimental data are in the low momentum region with $p \lesssim 1.7$GeV and no more constraints in the high momentum region. To study whether a different parametrization has an influence on the prediction we perform also calculations with two other parameterizations of the momentum-dependent potential, which give the same results in the low momentum region, but differ for high momenta, shown in the top panel of Fig. 3.2. The parameterization I (black dotted line) has the form of

$$V(\mathbf{p}, \mathbf{p}_1) = (a(\Delta p)^2 + b(\Delta p^4)) \exp[-c\Delta p]. \tag{3.2.7}$$

with $\Delta p = \sqrt{(\mathbf{p} - \mathbf{p}_1)^2}$. The parameterization II (blue dashed line) is the same as the parameterization I for momenta $\leq$ 2 GeV/c, but with a constant for momentum $>$ 2 GeV/c. The parameterization III (red solid line) for $\Delta p < 1.7$GeV is the same as the old one, while for $\Delta p > 1.7$ GeV/c, we take,

$$V(\Delta p) = d + e\Delta p + f\Delta p^2, \tag{3.2.8}$$

which gives a slight increase of the potential in the region of interest in this study. The parameters of the parameterization are shown in Table 3.1.

EoS	α [GeV]	β [GeV]	γ	K [MeV]
S	-0.3835	0.3295	1.15	200
H	-0.1253	0.071	2.0	380
SM	-0.478	0.4137	1.1	200
	a[GeV^{-1}]	b [GeV^{-3}]	c [GeV^{-1}]	
	236.326	-20.730	0.901	
	d[GeV]	e	f [GeV^{-1}]	
	72.237	27.085	-1.722	

Table 3.1: Parameters of the potential used in PHQMD assuming that the momenta are given in GeV/c.

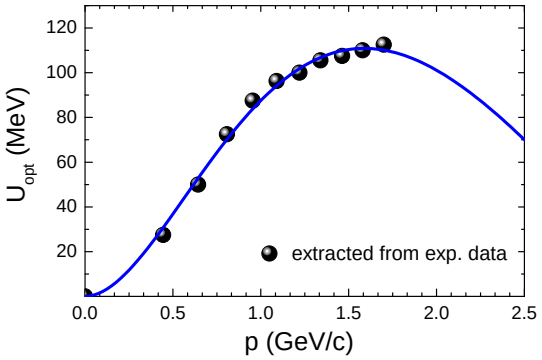

FIG. 3.2: Schrödinger equivalent optical potential U_{opt} versus total momentum p of the proton extracted from pA collisions [50].

For further details in the implementation of the momentum dependent potential in the QMD dynamics we refer to Refs. [30, 31].

3.3 Hadrons dynamics

The PHSD-PHQMD propagate hadronic and partonic degrees-of-freedom in time, including there interaction by potential interactions and scattering.

- **Time-space grid**

The calculations of mean fields, collisions, etc in PHSD are done using a 3D-grid of size 2 $\times$ 28 = 56 in each direction xyz. The size of the grid is 1 fm $\times$ 1 fm $\times 1/\gamma_{NN}$ fm = $2\Delta t$ respectively in xyz direction. The size of the grid in the z-direction is linearly increasing in time, as well as the time step Δt cf. Fig.3.3. The time step depends on collision energy and decreases with increasing energy. In PHQMD mode the limitation $\Delta t_{max} \leq 0.2$ fm/c is used. Then, the number of particles in each cells evolves smoothly in time.

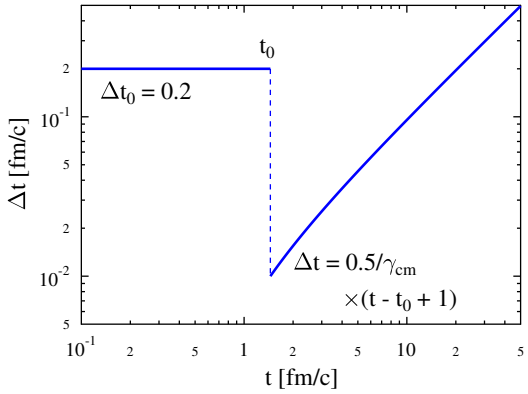

FIG. 3.3: Time step as a function of time evolution.

For the calculation of macroscopic quantities such as the elliptic flow v_2, one must run the code up to t_f = 500 fm/c to be sure to reach the kinetic freeze-out.

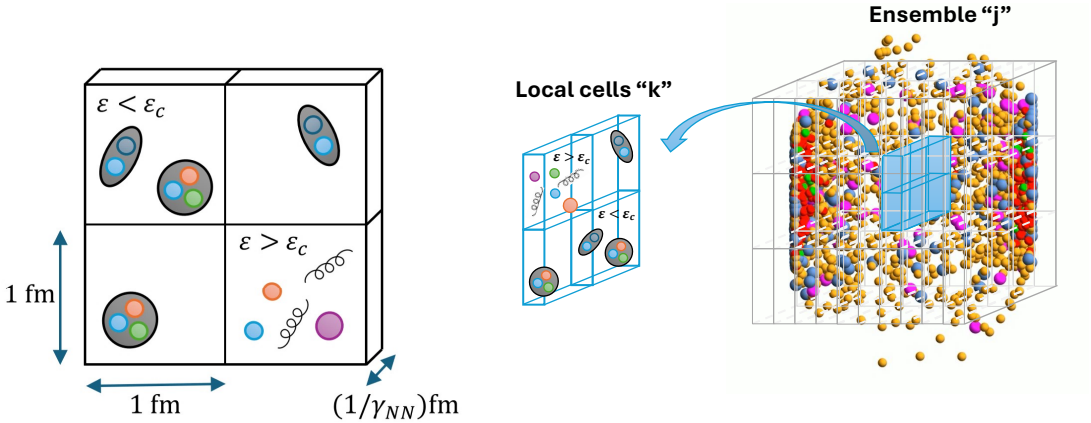

FIG. 3.4: Collisions and hadronization in cells depending on the local energy density ε, compared to the critical energy density ε_c = 0.4 GeV/fm^3.

- **Collisional criteria**

For collisions of 2 particles, we use `COLLCRIT(P1,P2,s,t,Deltat,IFL)` which is a standard geometrical collision citerion, according to the Kodama's prescription (in `GLUESCAT`).

- **Energy density**

The calculation of energy density, which is used for mean field and cross sections, is done for hadrons in the routine `EnDensETRANS()` (in file *Elocal.f*), and for partons in the routine `PADENS()` (in file *Elocal.f*).

The energy density for each cell is defined in the global computational frame - which is conventionally selected as the initial $N+N$ (nucleon-nucleon) center-of-mass frame:

$$\varepsilon = \frac{\sum_i E_i}{V_{cell}}, \tag{3.3.1}$$

where the sum of all particles in the cell is provided by $\sum_i$, and the volume of the cell is defined by $V_{cell} = \Delta x \Delta y \Delta z$ where $\Delta x = \Delta y = 1$ fm which is equal to the hadron size and Δz is time-dependent and adjusted dynamically as $\Delta z = 1/\gamma_{cm}$ fm for $t < t_0$ and $\Delta z = 1/\gamma_{cm} + (t - t_0)c$ fm for $t \geq t_0$, where t_0 is the touching time of the 2 colliding nuclei. Here $\gamma_{cm} = \sqrt{s_{NN}}/(2m_N)$, s_{NN} is the invariant energy of the N+N system.

The local energy density for each cell in the rest frame of the cell is computed using the velocity of this cell:

$$\vec{\beta} = \frac{\sum_i \vec{p}_i}{\sum_i E_i}, \tag{3.3.2}$$

which gives the Lorentz factor $\gamma = 1/\sqrt{1 - \vec{\beta}^2}$. Therefore, the local energy density of the cells is determined by

$$\varepsilon' = \frac{E'}{V'} = \frac{E/\gamma}{V \times \gamma} = \frac{\varepsilon}{\gamma^2}. \tag{3.3.3}$$

- **BB, mB, mm collisions**

In each time step, collisions are calculated with a loop over all parallel events inside collision subroutines. First for BB collisions, we use the routine `RELCOL()` (in *collis.f*) for all baryonic channels (Monte-Carlo over all possible processes). All collisions are done in the BB cms frame. The *calculational frame* is the cms frame for NN. For high energy scattering $\sqrt{s} > \sqrt{s_0} = 2.6$ GeV, we call the Lund string fragmentation routine `FRITZI()`. For low energy scattering $\sqrt{s} < \sqrt{s_0}$, $BB \to BB + m$ or $BB \to BB' \to BB + m$ collisions (including resonances), we call the routine `CROSW()` (in *cbuu.f*) for non-strange BB collision, or strangeness collision routines. Then for mesons, scattering (mm or mB) we use the routine `PIONDI()`.

For the meson-baryon collisions we use the routine `PIONAB()`. The test for collisions is done with two loops over mesons and baryons from the same parallel run (`NUM` and `ISUB`). As for BB collisions, we distinguish high energy scattering and low energy scattering. For $\sqrt{s} > \sqrt{s_0} = 2.6$ GeV we call `FRITZIPI()` (in *fritzi.f*) for $mB \to X$. For $\sqrt{s} < \sqrt{s_0} = 2.35$ GeV we call low energy routines (including strangeness production), for $mB \to B'$ or $mB \to mB$ (elastic or inelastic).

For energetic meson-meson collisions, $\sqrt{s} > \sqrt{s_0} = 1.3$ GeV, we call `FRITZI_mm()` (in *fritzi.f*) for $mm \to X$. Fow low energy mm collisions we use the routine `PIONCO()` (no

string excitation). This routine includes $mm \to m'$ (ex: $\pi\pi \to \rho$), and $mm \to mm$ (elastic or inelastic).

• **String models: FRITIOF & PYTHIA**

The primary string formation is calculated in the routine `RELCOL` (in *collis.f*). For secondary $B-B$, we call `FRITZI()`, for $m-B$ - l `FRITZIPI()` and for $m-m$ - `FRITZI_mm()`.

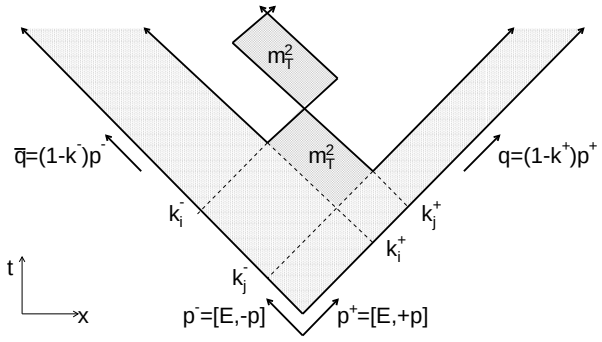

FIG. 3.5: Formation of hadrons from the Lund string picture.

• **Hadronic decays**

For all the hadronic decays (in *decays.f*), we use the decay width Γ taking into account in-medium effects, and we compute the decay probability:

$$\omega = \exp\left(-\frac{\Delta t \times \Gamma(M)}{\gamma \hbar c}\right), \tag{3.3.4}$$

with $\Gamma(M) = \Gamma_{vac}(M) + \Gamma_{coll}(\rho)$ and $\Gamma_{coll}(\rho) = \alpha \frac{\rho_B}{\rho_0}$.

• The spectral function of vector mesons (including in-medium effects) are calculated in the subrotines in file *sf_lib.f*. The subroutine `MASS_SF_DELTA()` (in *sf_lib.f*) defines the masses of Δ-resonances via Breit-Wigner spectral functions.

• **Formation time**

The **formation time** concept is applied in PHSD-PHQMD for the hadrons produced by string fragmentation. For the computation of the formation time, we use the routine `FORMA()` (in *collis.f*) for baryons and mesons. The normal "formed" hadrons have an identification number which is below 1000. For hadrons which are not yet formed, their identification number is increased by 1000. Hadrons are not formed if their formation time $\tau_f = 0.8$ fm/c ($t_f = \gamma\tau_f$ in calculational frame) is not reached. For example in BB initial hard collisions, the leading quarks and diquarks from the string are still prehadrons. When $t > t_f$ the pre-hadrons become hadrons and can collide and interact again.
We also consider as pre-hadrons the hadrons which are in the high density phase where the energy density ε is above the critical energy density $\varepsilon_c = 0.4$ GeV/fm^3. In the plasma phase, the hadrons can only decay.

• **Output for hadron/parton dynamics over time**

`StatTimeOut(time)` (in *pribig.f*) called in `main` gives statistics in time for baryons and mesons in output files *fort.310* and *fort.311*. This subroutine, also provides extended output for parton dynamics.

3.3.1 Baryon properties:

- ID(I,1) = type (+1000 if pre-hadron), anti-baryons get a negative sign,
- ID(I,2) = charge,
- ID(I,3) = last colliding partner,
- ID(I,4) = for resonances: how many times the meson was created,
- ID(I,5) = type of process from which the particle comes,
- ID(I,6) = abs: number of baryon collision; sign: target or projectile,
- ID(I,7) = strangeness content,
- ID(I,8) = 3 formed hadron; = 2 pre-hadron/leading baryon (have a formation time τ_f). Leading baryons are still allowed to interact with reduced cross sections:
  - $\sigma(q-B) = 1/3\ \sigma(BB) \approx 10$ mb,
  - $\sigma(qq-B) = 2/3\ \sigma(BB) \approx 20$ mb,
  - $\sigma(q-qq) = 2/9\ \sigma(BB) \approx 7$ mb.
- R(1-3,I) = coordinates x, y, z in fm,
- E(I) = mass (on/off-shell) in GeV,
- P(1-3,I) = momentum p_x, p_y, p_z in GeV,
- P(4,I) = production (creation) time,
- P(5,I) = individual formation time τ_f.

Description of ID(I,5) for baryons, which gives the reaction where the baryon was created, e.g.:

- = 200: string or non-string baryon formation from qqq,
- = 201: meson formation from qqq-string,
- = 220: hadronization from recombinaison (in RECOM).

The ID(I,5) is identical to IPI(I,5) of mesons (see below) if the both meson and baryon are the final particles.

3.3.2 Mesons properties:

- IPI(I,1) = type (+1000 if pre-hadron),
- IPI(I,2) = charge,
- IPI(I,3) = ID of the parent resonance of meson I
- IPI(I,4) = how many time the meson was created (+ for π, − for η),
- IPI(I,5) = type of the parent resonance (ID(IPI(I,3)),1)) or reaction (see list below),
- IPI(I,6) = recording of kaons channel,
- IPI(I,7) = strangeness content,
- IPI(I,8) = 3 final meson; else quark or antiquark; = 1: leading mesons (IPI(I,1) ¡ 1000),
- RPI(1-3,I) = coordinates x, y, z in fm,
- PPI(1-3,i) = momentum p_x, p_y, p_z in GeV,
- PPI(4,i) = energy (on/off-shell) in GeV,
- PPI(5,i) = production (creation) time,

- `PPI(6,i)` = `PPI(8,i)` = baryon density at creation time,
- `PPI(7,i)` = individual formation time τ_f.

3.3.3 Production channels for mesons and baryons `IPI(I,5)`, `ID(I,5)`

`IPI(I,5)`, `ID(I,5)` provides information about the production channel, i.e. the reactions in which the hadron was created.
Notations: $K = (K^+, K^0, K^{+\star}, K^{0\star})$ and $\tilde{K} = (K^-, \bar{K}^0, K^{-\star}, \bar{K}^{0\star})$;
$V = (\rho, \omega, \phi)$ - vector mesons.

=1 elastic scattering of baryons
=4 from η'-decay
=5 from ϕ-decay
=6 from ω-decay
=7 from K^*-decay
=8 π from ρ-decay
=9 ρ from $\pi + \pi \to \rho$, or ϕ from $K + \bar{K} \to \phi$
=10 $\pi + \pi \to K + \bar{K}$
=11 $N + N \to N + N + K + \bar{K}$
=12 $\pi + N \to N + K + \bar{K}$
=12+1000=1012: $\pi + \Delta \to N + K + \bar{K}$
=13 $N + N \to N + Y + K$
Replacement of =17 at low energies with g-matrix (jkaongmatr.ge.2)
=13 +5000=5013: $\Delta + \Delta \to \Delta + Y + K$
=13 +4000=4013: $N + \Delta \to \Delta + Y + K$
=13 +3000=2013: $N + N \to \Delta + Y + K$
=13 +2000=2013: $\Delta + \Delta \to N + Y + K$
=13 +1000=1013: $N + \Delta \to N + Y + K$
=14 a_1 from $\pi + \rho \to a_1$
=15 ϕ from $\pi + \rho \to \phi$

3-body (optionally):

=16 $N + N \to N + N + \pi$
=-16 $N + N + \pi \to N + N$

Strings:

=17 BB-string
=18 MM-string or string from $B\bar{B}$-annihilation
=-18 string from $B\bar{B}$-annihilation
=19 MB-string

Hadronic reactions and decays:

=20 $K + N \to \pi + Y$
=21 $\pi + Y \to K + N$

=22 $\pi + N \to K + Y$
=22 +1000=1022: $\pi + \Delta \to K + Y$
=23 $\Lambda + \eta \to \Xi + K$
=24 $\Xi + K \to \Lambda + \eta$
=25 $K + Y \to \pi + N$
=26 $K + \bar{K} \to \pi + \pi$
=27 $K + \pi \to K^*$
=28 $a_1 \to \pi + \rho$
=29 $m + Y \to K + \Xi$

=30 η from $NN \to \eta + NN$ (from Lund)
=31 ϕ from $NN \to \phi + NN$ (from Lund)
=32 $\eta + M \to \phi + \pi$
=34 $\pi + K^* \to K^*(1400)$

=36 $\bar{K} + Y \to \pi + \Xi$
=37 $K^*(1440) \to K^* + \pi$ decay
=39 $\bar{K} + \Xi \leftarrow \pi + \Omega$
=40 η' decay: $\eta' \to 2\pi + \eta$ or $\eta' \to \rho + \gamma$
=47 a_0 decay(IPI(I,1)=-2), effective resonance, optionally
=56 elastic scattering of strange baryons $Y + B$

=60 vector meson production by low energy BB collisions $BB \to V + BB$, where $V = \rho, \omega, \phi$
=61 ρ meson production by low energy BB collisions via $N + N \to N(1520) + N \to \rho + N + N$
=62 vector meson production by low energy mB collisions $m + B \to V + B$, where $V = \rho, \omega, \phi$
=63 ρ meson production by low energy mB collisions via $\pi + N \to N(1520) \to \rho + N$
=64 ϕ from $\eta + N \to \phi + N$
=65 ϕ from $\rho + B \to \phi + N$
=77 from effective κ decay (optionally)

m+B channels:
=85 elastic $\pi N \to \pi N$
=88 η from eta's from $\pi^- + n \to \eta + \Delta^-$ channel
=89 η from $\pi^- + p \to \eta + n$ channel
=91 $\eta + N \to N(1535)$
=92 $\omega + N \to \pi + N$
=93 $\omega + N \to N$
=94 $\rho + N \to \pi + N$
=95 $\rho + N \to N$ (in-medium rho: $Mrho < mpi$)
=96 $\pi + N \to \pi + \pi + N$ via 3 body (optionally)
=-96 $\pi + \pi + N \to \pi + N$ via 3body
=97 elastic $V + N \to V + N$, $V = \rho, \omega$

=98 $\pi + N \to$ Baryon Resonance

3 mesons annihilation to $B + \bar{B}$ channels:

=100 3 mesons $\to$ B+Bbar

strange baryon scattering:

=101 $\Lambda + \Lambda \to p + \Xi^-$
=102 $\Lambda + \Lambda \to n + \Xi^0$
=103 $\Lambda + \Sigma^+ \to p + \Xi^0$
=104 $\Lambda + \Sigma^- \to n + \Xi^-$
=105 $\Lambda + \Sigma^0 \to p + \Xi^-$
=106 $\Lambda + \Sigma^0 \to n + \Xi^0$
=107 $\Sigma^0 + \Sigma^0 \to p + \Xi^-$
=108 $\Sigma^0 + \Sigma^0 \to n + \Xi^0$
=109 $\Sigma^+ + \Sigma^- \to p + \Xi^-$
=110 $\Sigma^+ + \Sigma^- \to n + \Xi^0$
=111 $\Sigma^+ + \Sigma^0 \to p + \Xi^0$
=112 $\Sigma^0 + \Sigma^- \to n + \Xi^-$
=121 $\Lambda + \Sigma \leftarrow N + \Xi$
=122 $\Lambda + \Sigma^- \leftarrow n + \Xi^-$
=123 $\Sigma + \Sigma \leftarrow N + \Xi$
=124 $\Sigma^0 + \Sigma^- \leftarrow n + \Xi^-$
=125 $\Lambda + \Lambda \leftarrow n + \Xi^0$
=126 $\Lambda + \Lambda \leftarrow p + \Xi^-$
=127 $\Lambda + \Sigma^0 \leftarrow n + \Xi^0$
=128 $\Lambda + \Sigma^0 \leftarrow p + \Xi^-$
=129 $\Sigma^0 + \Sigma^0 \leftarrow n + \Xi^0$
=130 $\Sigma^0 + \Sigma^0 \leftarrow p + \Xi^-$
=131 $\Sigma^+ + \Sigma^- \leftarrow n + \Xi^0$
=132 $\Sigma^+ + \Sigma^- \leftarrow p + \Xi^-$

from decay of baryon resonances:

= 141 - 159 from decay of baryonic resonances in PIONEM with ID1:
IPI(I,5)=150+ID(J,1) where ID1=-9 ($\bar{\Xi}^*$) till 9 (Ξ^*)
The most important decay channels:
= 152 - Δ decay
= 153 - N(1440)
= 154 - N(1535)
= 157 - Σ^*
= 159 - Ξ^*

reactions with charm hadrons:

=160 charm from hard NN collisions
=161 $D + B \to \Lambda_c + \pi$

Strangeness channels from RELCOL:

IPI(I,5)= ID(I,5) = IPTYPE
= 171 $NN \to N\Lambda K^+$
= 172 $NN \to N\Sigma K^+$
= 173 $N\Delta \to N\Lambda K^+$
= 174 $N\Delta \to N\Sigma K^+$
= 175 $\Delta\Delta \to N\Lambda K^+$
= 176 $\Delta\Delta \to N\Sigma K^+$

Channels with deuterons:

= 1101 $N + N + \pi \to d + N$
= -1101 $d + N \to N + N + \pi$
= 1301 $N + N + N \to d + N$
= -1301 $d + N \to N + N + N$

** Channels with photons (active only optionally with IPHOTON=1):

= 40 $m + m \to m + m + \gamma$
= 50 $\pi + \pi \to \rho + \gamma$
= 51 $\omega \to \pi_0 + \gamma$
= 60 $\pi + \rho \to \pi + \gamma$
= 70 $\omega \to \pi^0 + \gamma$,
= 80 η from ϕ-decay : $\phi \to \eta + \gamma$
= 90 $a_1 \to \pi + \gamma$

elastic $m + B$, $m + m$ scattering:

=190 elastic $m + B$ collisions in FRITZIPI
=191 elastic $m + m$ collisions in PIONCO
=192 elastic $m + m$ scattering from FRITZI_MM

from partonic phase - QGP:

=200 non-string meson formation from qq
=201 meson formation from qq-string
=220 from RECOM
=99 'quasiparticle' ρ-meson from $\pi+\pi$, $\pi+K$ annihilation - used for hadron dissolution to QGP only

from G-matrix:

=-100 elastic
=-100+ich for different incoming channels:
=-99 ich=1 $K^- p$
=-98 ich=2 $\bar{K}^0 n$
=-97 ich=3 $\pi^0\Lambda$
=-96 ich=4 $\pi^0\Sigma^0$
=-95 ich=5 $\eta\Lambda$
=-94 ich=6 $\eta\Sigma^0$
=-93 ich=7 $\pi^+\Sigma^-$
=-92 ich=8 $\pi^-\Sigma^+$

=-91 ich=9 $K^+\Xi^-$
=-90 ich=10 $K^0\Xi^0$
=-89 ich=11 K^-n
=-88 ich=12 $\pi^0\Sigma^-$
=-87 ich=13 $\pi^-\Sigma^0$
=-86 ich=14 $\pi^-\Lambda$
=-85 ich=15 $\eta\Sigma^-$
=-84 ich=16 $K^0\Xi^-$

3.3.4 Extended information on collision history

Output of kaon statistics from field `kprod`, for production:

- `kprod(1,-1)=` K from BB-string,
- `kprod(1,1)=` $\tilde{K}$ from BB-string,
- `kprod(2,-1)=` K from mB-string,
- `kprod(2,1)=` $\tilde{K}$ from mB-string,
- `kprod(3,-1)=` should be 0,
- `kprod(3,1)=` $\tilde{K}$ from $\Upsilon + \pi \to K + N$,
- `kprod(4,-1)=` K from $N + \pi \to \Upsilon + K$,
- `kprod(4,1)=` should be 0,
- `kprod(5,-1)=` K from $m + m \to K + \tilde{K}$,
- `kprod(5,1)=` $\tilde{K}$ from $m + m \to K + \tilde{K}$,
- `kprod(6,-1)=` K from $B\bar{B}$ annihilation,
- `kprod(6,1)=` $\tilde{K}$ from $B\bar{B}$ annihilation,
- `kprod(7,-1)=` K from ϕ-decay,
- `kprod(7,1)=` $\tilde{K}$ from ϕ-decay,

and for absorption:

- `kprod(-2,-1)=` K absorption from mB-string,
- `kprod(-2,1)=` $\tilde{K}$ absorption from mB-string,
- `kprod(-3,-1)=` K absorption from $K + N \to \Upsilon + \pi$,
- `kprod(-3,1)=` $\tilde{K}$ absorption from $\tilde{K} + \Upsilon \to N + \pi$.

Possible state of the parameter `gpa`:

- `gpa(1)` : rescattering on/off,
- `gpa(2)` : time step size: = 1 fixed time step resc(1); = 2 dynamical time step size, parameters `resc(2)`, `resc(3)`,
- `gpa(3)` : calculation and output of density on/off,
- `gpa(4)` : `RELCOL` on/off,
- `gpa(5)` : Fermi motion in/out,
- `gpa(7)` : J/Ψ production on/off,
- `gpa(8)` : string fragmentation on or off (0 or 1),
- `gpa(9)` : meson scattering on or off (1 or 0)(default=1),
- `gpa(10)`: meson-meson scattering on or off (1 or 0)(default=1),

- gpa(11): annihilation on/off (default=1),
- gpa(12): momentum output of p, π, K at the end [0/1] ?,
- gpa(13): $\rho + \pi \to a_1/\phi$ included/excluded [1/0],
- gpa(14): production or $B\bar{B}$-pairs from mm-collisions on/off [1/0],
- gpa(15): elastic $\pi\pi$ scattering,
- gpa(16): grid size in z-direction: $1 \to dz = 1$; $2 \to dz = 1/\gamma_{cm}$,
- gpa(22): number of different string radii in 0.1 fm steps starting from resc(22),
- gpa(40): $3D$-plot output for Mathematica, only if NUM=1.

Possible state of the parameter resc:

- resc(1) : time step size for gpa(2)=1 (default 0.2),
- resc(2) : time step size for gpa(2)=2 during high density phase: dt = resc(2)$/\gamma_{cm}$ (default 0.5),
- resc(3) : time step size for gpa(2)=2 during formation phase: dt = resc(2)$/\gamma_{cm}$ (default 2.0),
- resc(4) : max. impact parameter for $\pi + N$ in fm (default 4.0),
- resc(5) : max. impact parameter for $m + m$ in fm (default 2.0),
- resc(6) : low energy ϕ absorption cross-section (5.0 mb),
- resc(7) : low energy ρ absorption cross-section (10.0 mb),
- resc(8) : low energy η' absorption cross-section (10.0 mb),
- resc(9) : low energy ω absorption cross-section (10.0 mb),
- resc(10): fraction of $\tilde{K}N \to \Lambda$ of the total $\tilde{K}$ absorption cross-section. (default value: 0.2),
- resc(11): fraction of $\tilde{K}N \to \Sigma$ of the total $\tilde{K}$ absorption cross-section. (default value: 0.15),
- resc(12): $c\bar{c}N$ absorption cross-section in mb (default 6.0 mb),
- resc(13): $J/\Psi N$ absorption cross-section in mb (default 3.0 mb),
- resc(14): formation time $c\bar{c} \to J/\Psi$ in fm (default 0.3 fm),
- resc(15): b_{max} for $nn \to J/\Psi$ in fm (default=1.0),
- resc(17): impact parameter for $mm \to B\bar{B}$ in fm, (gpa(14)=1),
- resc(18): cross-section for $mm \to K\tilde{K}$ in mb (for each isospin-chanal),
- resc(19): string threshold BB in GeV,
- resc(20): string threshold mB in GeV,
- resc(21): 'formation time' for J/Ψ in fm (default -1.5),
- resc(22): minimal string-radius for J/Ψ absorption,
- resc(23): elastic cross section for baryon meson,
- resc(40): time step size of output for Schertler movie.

Internal parameter in RELCOL and PIONAB:

- IBLOCK = 0, nothing has happened,
- IBLOCK = 1, elastic nn collision,
- IBLOCK = 2, $n + n \to n + \Delta$,
- IBLOCK = 3, $n + \Delta \to n + n$,
- IBLOCK = 4, $n + n \to n + N^\star$,

- IBLOCK = 5, $n + N^{\star} \rightarrow n + n$,
- IBLOCK = 6, $n + n \rightarrow n + N^{\star 2}$,
- IBLOCK = 7, $n + N^{\star 2} \rightarrow n + n$,
- IBLOCK = 8, $n + \Delta \rightarrow n + N^{\star 1}$,
- IBLOCK = 9, $n + N^{\star 1} \rightarrow n + D$,
- IBLOCK =10, $n + \Delta \rightarrow n + N^{\star 2}$,
- IBLOCK =11, $n + N^{\star 2} \rightarrow n + D$,
- IBLOCK =12, $n + N^{\star 1} \rightarrow n + N^{\star 2}$,
- IBLOCK =13, $n + N^{\star 2} \rightarrow n + N^{\star 1}$,
- IBLOCK =14, $\Delta + \Delta \rightarrow n + N^{\star 1}$,
- IBLOCK =15, $\Delta + \Delta \rightarrow n + N^{\star 2}$,
- IBLOCK =16, $n + n \rightarrow n + n + \pi$ s-state,
- IBLOCK =17, string fragmentation.

Identification of hadrons in (P)HSD, see the routines in *fritzi.f*:

- TRANSPOSECODE() to convert from (P)HSD to LUND using KFHSD(ID1,ID2)= number in LUND (e.g. KFHSD(1,1)= 2212 is the proton),
- HSDID() to convert from LUND to (P)HSD using the number from LUND to ID1+1000.

Chapter 4

Quark-Gluon Plasma

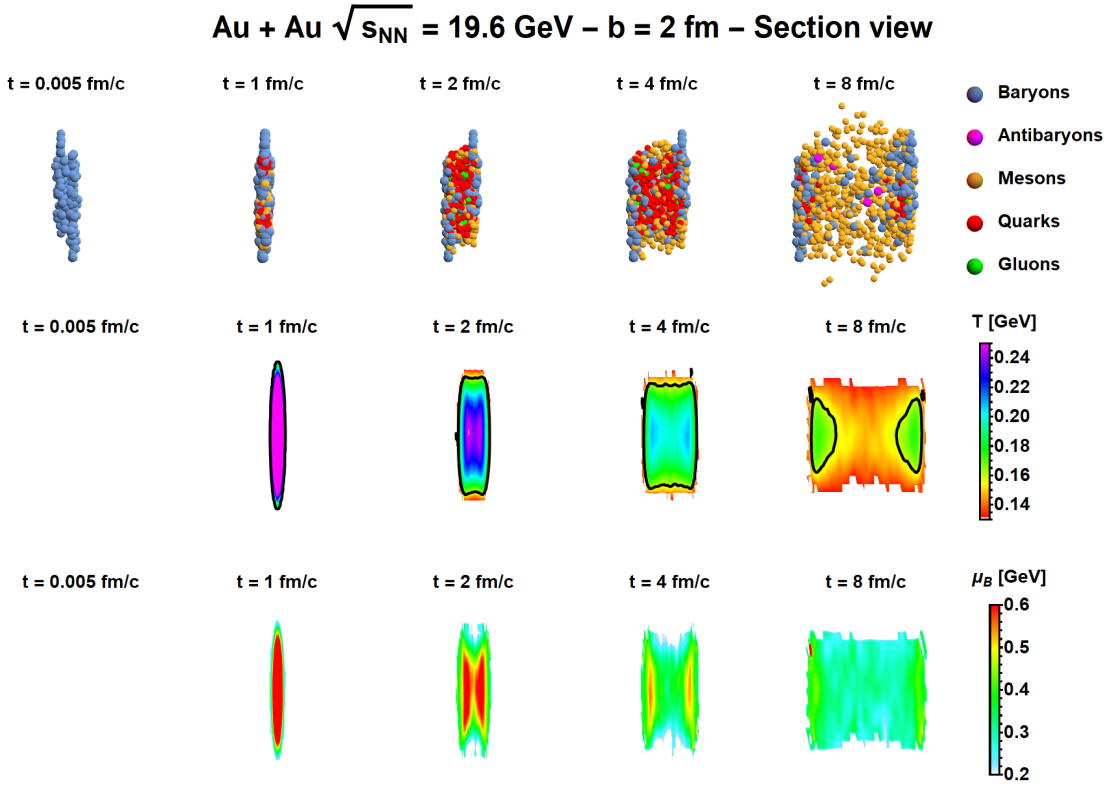

FIG. 4.1: Illustration of the time evolution of central Au+Au collisions (upper row, section view) at a collisional energy of $\sqrt{s_{NN}} = 19.6$ GeV within the PHSD [?]. The local temperature T (middle row), baryon chemical potential μ_B (lower row), as extracted from the PHSD for $y \approx 0$. The black lines (middle row) indicate the critical temperature $T_c \simeq 0.158$ GeV. The figures are adopted from [51].

For the evolution of the partonic systems at lower bombarding energies $\sqrt{s_{NN}}$ energies – where the baryon chemical potential, μ_B, is finite – the PHSD approach has been extended (versions 5.x and above) to incorporate partonic quasiparticles and their differential cross sections that depend not only on temperature T(or ϵ) as in the PHSD studies at RHIC and LHC energies, but also on the chemical potential μ_B explicitly.
We have considered the following three settings for the transport simulations:

- **PHSD4.x**: the masses and widths of quarks and gluons depend only on T. The cross sections for partonic interactions depend only on T as evaluated in the 'box' calculations in Ref. [40] in order to merge the QGP interaction rates from all possible partonic channels to the total temperature-dependent widths of the DQPM propagator.
- **PHSD5.x - μ_B**: the masses and widths of quarks and gluons depend on T and μ_B explicitly; the differential and total partonic cross sections are obtained by calculations of the leading order Feynman diagrams from the DQPM and explicitly depend on the invariant energy $\sqrt{s}$, temperature T and baryon chemical potential μ_B. This is realized in the full version of PHSD5.x
- (not default) **PHSD5.x - $\mu_B = 0$** : the masses and widths of quarks and gluons depend only on T; however, the differential and total partonic cross sections are obtained by calculations of the leading order Feynman diagrams employing the effective propagators and couplings $g^2(T/T_c)$ from the DQPM at $\mu_B = 0$ [3]. Thus, the cross sections depend explicitly on the invariant energy of the colliding partons $\sqrt{s}$ and on T. This is realized in the PHSD5.x by keeping $\mu_B = 0$ (set `ievalmuB=0` in *main.f*).

Main parameters:

- `iDQPM` = 0 used for PHSD4.X, = 1 used for latest PHSD5.X with T, μ_B for QGP - corresponds to the latest version of DQPM2021, 2 - DQPM2015(PHSDv5 from 2019).
- `ievalmuB` = 1 by default for PHSD5.X (in *main.f*)

4.1 Extraction of temperature and chemical potential

In the transport approach, T and μ_B are not natural observables, however, one can determine the energy density and baryon density in each cell. In order to extract T and μ_B from the corresponding EoS of the partonic system one has to solve the following system of equations [3]:

$$\begin{cases} \epsilon^{\rm EoS}(T,\mu_B) = \epsilon^{\rm PHSD}/r(x) \\ n_B^{\rm EoS}(T,\mu_B) = n_B^{\rm PHSD}. \end{cases} \tag{4.1.1}$$

Here the left-hand sides consist of the energy density and baryon density from the lQCD Taylor expansion method, which depends on the unknown T and μ_B. The right-hand sides of these equations represent the energy density and baryon density evaluated in PHSD. In Eq. (4.1.1) the energy density from PHSD $\epsilon^{\rm PHSD}$ is divided by the function

$r(x)$, which reads

$$r(x) = \begin{cases} \frac{x^{-1/3}}{2}\left[1 + \frac{x\ \mathrm{arctanh}\sqrt{1-x}}{\sqrt{1-x}}\right] & \text{for } x \leq 1 \\ \frac{x^{-1/3}}{2}\left[1 + \frac{x \arctan\sqrt{x-1}}{\sqrt{x-1}}\right] & \text{for } x \geq 1 \end{cases} . \tag{4.1.2}$$

Here the anisotropy parameter x is approximated as a function of the pressure components as $x = (P_\parallel/P_\perp)^{3/4}$. $r(x)$ accounts for the momentum anisotropy of the considered cell according to the shape generalized equation of state developed in Ref. [52].

File Tmunu.f

```
SUBROUTINE TMUNUPM(Tcoll,TIME,iwrite,ichange,ileading,iformed,
                   ithermal,ievalmuB)
```

Purposes:

- To calculate the energy momentum tensor (based on `TAKESHI()`) and its eigenvalues and eigenvector corresponding to the energy density in each cell and each time step w/o leading hadrons.
- if `ichange=0` - old calculation of energy density for bulk dynamics
- presently - only `PPARTON(9,I)` is changed, (not the whole `PATTR`) however, `PATTR()` later is using `PPARTON(9,I)`, so the QGP parton density is updated in `PATTR()` also, but the hadronic part of `PATTR()` is still from `ETTR(IX,IY,IZ)`.
- w/o leadings

Optional output files:

- if `iwrite=1`, write all $T^{\mu\nu}$ in `Tmunu_muB.dat`
- `Nparticles_t.dat` `#time-Tcoll,nparton,nbaryon,nmeson`
- `isnap=1` Energy density fraction of QGP w/o leadings `QGP_energy_fraction.dat`.

4.2 Dynamical QuasiParticle Model

In the partonic phase the properties of quarks and gluons are described in terms of strongly interacting quasiparticles within the Dynamical Quasiparticle Model (DQPM) [11, 3]. The DQPM provides an effective description of the nonperturbative quark–gluon plasma (QGP) by matching the thermodynamic properties of quasiparticles to lattice QCD results for the equation of state [3]. This approach allows one to determine effective masses, widths, and interaction rates of quarks and gluons as functions of temperature and baryon chemical potential.

The parametrisation of masses,widths and spectral functions are contained in the DQPM module (file `DQPM.f`).

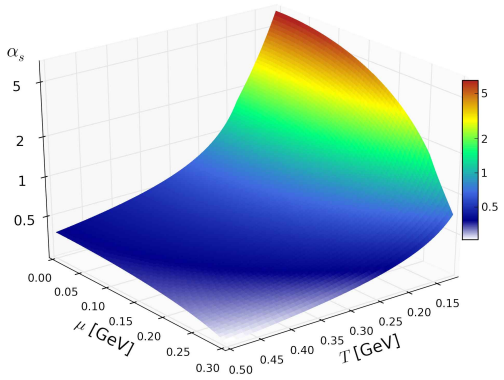

FIG. 4.2: Coupling constant $\alpha_s = \dfrac{g^2}{4\pi}$ in the Dynamical QuasiParticle Model.

The elastic cross-sections are evaluated in the beginning of the calculations and stored in a table. All routines are located on `DQPM.f` There are 2 main versions of parametrizations in the subroutine (1, 0)

for PHSD versions $\leqslant 4$:

- `iDQPM = 0` - DQPM2014 parameterizations

for PHSD versions $\geqslant 5$:

- `iDQPM = 1` - latest DQPM2021 with the strangeness neutrality $< n_s >= 0$
- `iDQPM = 2` - DQPM2015 as implemented in PHSD5.0 (2019)
- `iDQPM = 3, 4` - DQPM2014, pDQPM old p-dependence parametrizations (not used)

4.2.1 Potentials for the partonic evolution

All parametrizations for the potential energy density V[GeV/fm^3] are located in the subroutine `POTT(mu_B,RHOP,POTER,FITP,PSACL,UMV,UMS,IV)` V $\rightarrow$ POTER. For the updated PHSD5.x version from 2022 we employ the following parametrization of the potential [in GeV]:

$$V_{dqpm}(\rho_s, \mu_B) = v_1(\mu_B)\rho_s^{v_2(\mu_B)} + v_3(\mu_B)\rho_s + v_4(\mu_B) \tag{4.2.1}$$
$$v_1(\mu_B) = 2.30738\mu_B^{2.6934} + 1.43158 \tag{4.2.2}$$
$$v_2(\mu_B) = -0.0961343\mu_B^{1.94121} + 1.20579 \tag{4.2.3}$$
$$v_3(\mu_B) = -2.65452\mu_B^{2.59192} - 0.671792 \tag{4.2.4}$$
$$v_4(\mu_B) = -0.027843\mu_B^2 + 0.11667 \tag{4.2.5}$$
$$\tag{4.2.6}$$

previous versions:

- DQPM15 PHSD5.0: $V = 0.19\rho_p + 0.12\rho_p^{1.48}$,
- DQPM14 PHSD4.x: $V = 0.4\rho_p + 0.333/1.45\rho_p^{1.45}$

In scalar potential U_s[GeV] $U_s = dV/d\rho_s$ is parametrized as function of the scalar density $\rho_s[1/fm^3]$ and μ_B.

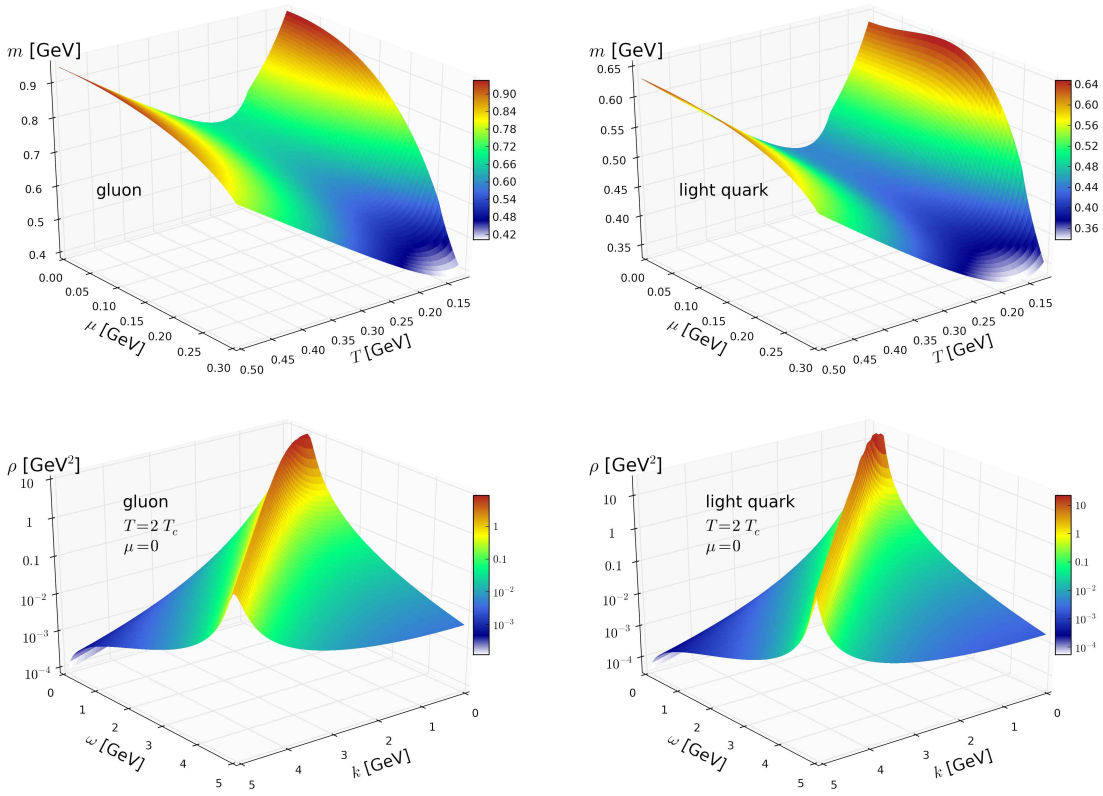

FIG. 4.3: Masses and spectral function of quarks and gluons in the Dynamical QuasiParticle Model.

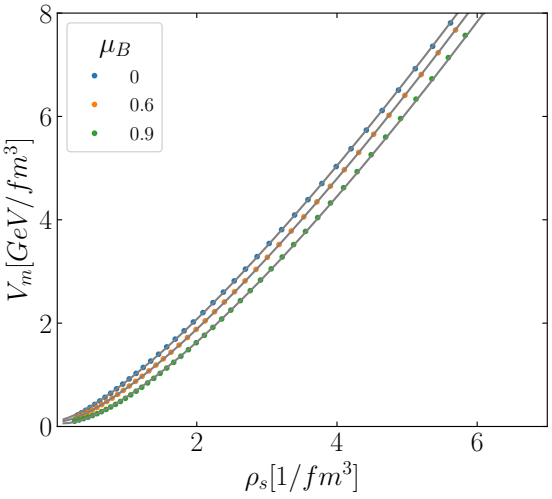

FIG. 4.4: DQPM 21 potential energy density as a function of the scalar density for the QGP phase at different μ_B in GeV.

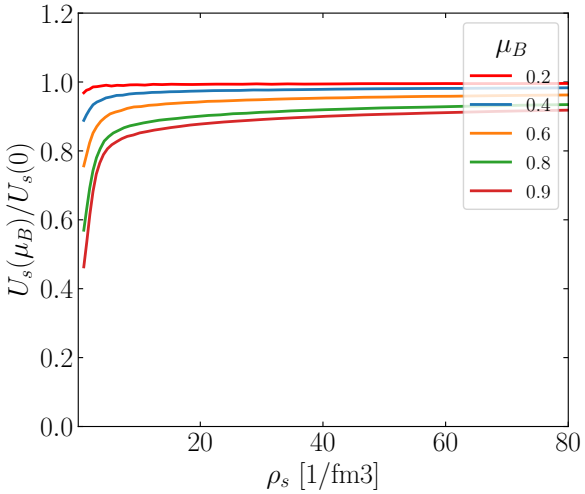

FIG. 4.5: DQPM 21 MF scalar potential as a function of the scalar density for the QGP phase at different μ_B in GeV.

4.3 Strong interaction

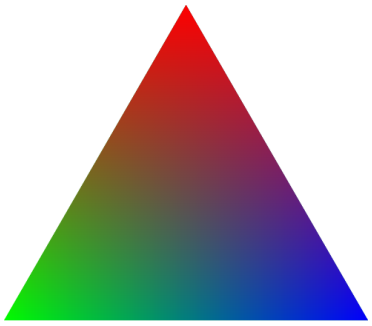

Description of meson production channels from the parton phase:
`IPI(I,5)`:

= 200 – non-string meson formation from $q\bar{q}$
= 201 – meson formation from $q\bar{q}$-string
= 99 – 'quasiparticle' ρ-meson from $\pi + \pi$ annihilation

`ID(I,5)`:

= 200 – string OR non-string baryon formation from qqq
= 201 – baryon formation from qqq-string

4.4 Partonic vectors in the PHSD

Partons properties:

- `IPARTON(I,1)` = type, anti-particles get a negative sign,
- `IPARTON(I,2)` = charge,
- `IPARTON(I,3)` = color $(1, 2, 3, -1, -2, -3)$,

- `IPARTON(I,4)` = last colliding partner,
- `IPARTON(I,5)` = for (anti-)quark: production channel; for gluon: second color,
- `RPARTON(1-3,I)` = coordinates x, y, z in fm,
- `PPARTON(1-3,I)` = momentum p_x, p_y, p_z in GeV,
- `PPARTON(4,I)` = energy (off-shell) in GeV,
- `PPARTON(5,I)` = local energy density at creation time,
- `PPARTON(6,I)` = individual formation time $\tau_f = E\hbar c/m_T^2$.

4.5 Hadronization

The subroutine `DISSOLVE()` (in *parton.f*) is used for the formation of the partonic phase. It is a loop over all hadrons (baryons and mesons) which select only the pre-hadrons (ID > 1000) but excluding leading baryons for a dissolution: $m \to q\bar{q}$ and $B \to qqq$. Then, it calls the routines `POTRAT()`, which gives the local scalar density ρ_s (Lorentz invariant) of the partons, which is then used in the routine `MEANF()` which gives masses m and width Γ values for the formed partons.

The color charge of partons and diquarks is considered through the following combination diagram:

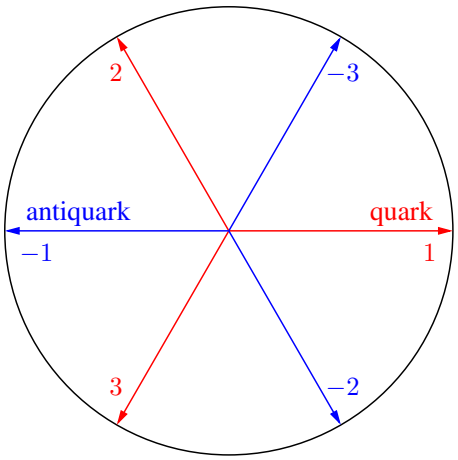

For instance, a diquark composed of two quarks of charge 2 and 3 gets an equivalent charge of -1.

The routine `POTRAT()` determines the ratio of potential energy to total energy from the DQPM model. This routines separates time-like energy of quasiparticles from space-like potential energy density. For this purpose, one computes the mean field as:

$$\mathcal{U}_s = \frac{\partial V_q}{\partial \rho_s}, \tag{4.5.1}$$

which gives the scalar force on the particle:

$$\frac{m_q}{E_q}\frac{\partial \mathcal{U}_s}{\partial \rho_s}\underbrace{\frac{\partial \rho_s}{\partial \vec{r}}}_{\vec{\nabla}\rho_s} = \frac{m_q}{E_q}\underbrace{\vec{\nabla}\mathcal{U}_s}_{\vec{F}}. \tag{4.5.2}$$

This force usually accelerates particles (repulsive potential from DQPM). This effect plays a role in the pressure formation which forms the elliptic flow v_2.

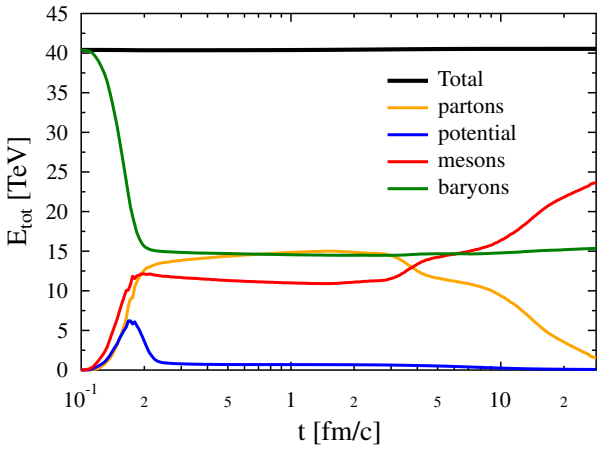

FIG. 4.6: Evolution of the fraction of energy in the system among different species from file *fort.485*.

The routine `HADRONS()` (in *main.f*) is used for meson formation. For instance we use the energy of quark and antiquark:

$$\begin{aligned} p_q^0 &= \sqrt{\vec{p}^2 + (m_q + \mathcal{U}_s)^2} \\ p_{\bar{q}}^0 &= \sqrt{\vec{p}^2 + (m_{\bar{q}} + \mathcal{U}_s)^2}. \end{aligned} \tag{4.5.3}$$

The different energy components are written out on `unit=485` (see Fig. 4.6).

The hadronization is done when the energy density decreases bellow the critical value of `ENCUT` = 0.75 GeV/fm^3. The dissolution of hadrons is the opposite process, but the critical value is 0.5 GeV/fm^3, in order to avoid a "yo-yo" effect in the cells. The radius of hadronization (to look for a partner) is `RCUT` = 0.67 fm.

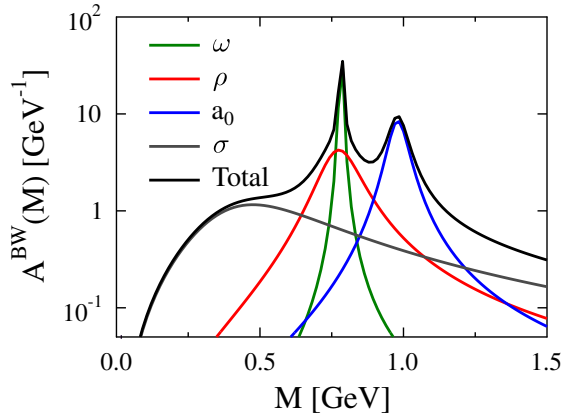

FIG. 4.7: Resonance spectrum for Breit-Wigner distributions for some vector mesons.

Broad resonances allow hadronization of heavy quarks from DQPM. For mesons ($q\bar{q} \rightarrow M$) there are 25 different possible combinations (with weight ω_i). There are 7 combinations for baryons ($qqq \rightarrow B$). In total, we have 32 possible channels ($[\omega_1,\omega_2,\ldots,\omega_{32}]$). In practice, the most common way to hadronize is: $q\bar{q} \rightarrow$ Res. $\rightarrow \pi\pi$ or $\pi\pi\pi$.

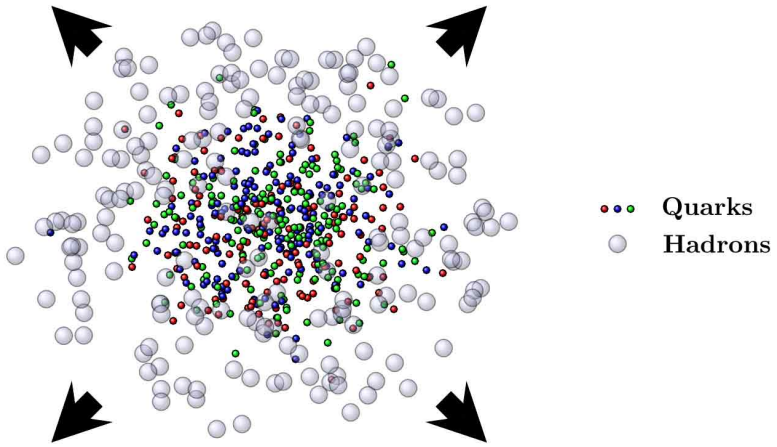

Table 4.1: The **partons** identification codes.

IPARTON(j,1)	type	Charge
1	u	2/3
2	d	-1/3
3	s	-1/3
4	uu	4/3
5	dd	-2/3
6	ud	1/3
7	ss	-2/3
8	us	1/3
9	ds	-2/3
10	gluon	0
11	c	2/3
12	b	-1/3

4.6 Ratqgp for Event Analysis: Ratio of the QGP after the hadronization

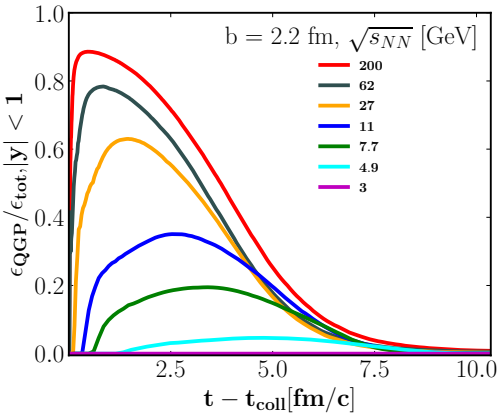

FIG. 4.8: The QGP energy fraction from the PHSD as a function of time in central (impact parameter $b = 2.2$ fm) Au+Au collisions for different $\sqrt{s_{NN}} = 200 - 3$ GeV at midrapidity $|y| < 1$.

In our previous discussions, we focused on the ratio of energy density, which is averaged over different events, specifically its variation over different collision energies as a function of time. Figure 4.8 illustrates this concept in detail for different $\sqrt{s_{NN}} = 200 - 3$ GeV

We are now introducing a new metric, R_i, which is uniquely defined for each event. The primary purpose of R_i is to quantify the extent of the QGP influence during an event. This parameter is formulated based on the intrinsic properties of individual events for each event which depends only on the event properties and can describe how much QGP was contained during the whole event.

- higher values of R_i are indicative of a more pronounced influence of QGP
- R_i is written in the *phsd.dat* file

A more pronounced influence of the QGP is evident in various results, such as an increased production of baryons and strange particles and variations in flow observables.

$$R_i = \int_0^{t_F} dt \frac{E_i^{QGP}(t)}{E^{tot}(t)} \tag{4.6.1}$$

In this equation, $R_i[fm/c]$ represents a weight for the QGP, E_i^{QGP} is the QGP fraction as a function of time from hadronization, and E^{tot} stands for the total energy.

Here for each event, we evaluate as $E_i^{QGP} = \sum_j E_i^j$, by summing over the energies of individual hadrons - mesons and baryons after the successful hadronization in `HADRONIZATION()` (in *parton.f*).

Typical values R_i for most central events Au+Au collisions at different energies $\sqrt{s_{NN}}$:

- 200 GeV: $(0.16 - 0.3)$ fm/c
- 27 GeV: $(0.04 - 0.07)$ fm/c

- 5 GeV: $(0.14 - 0.03)$ fm/c

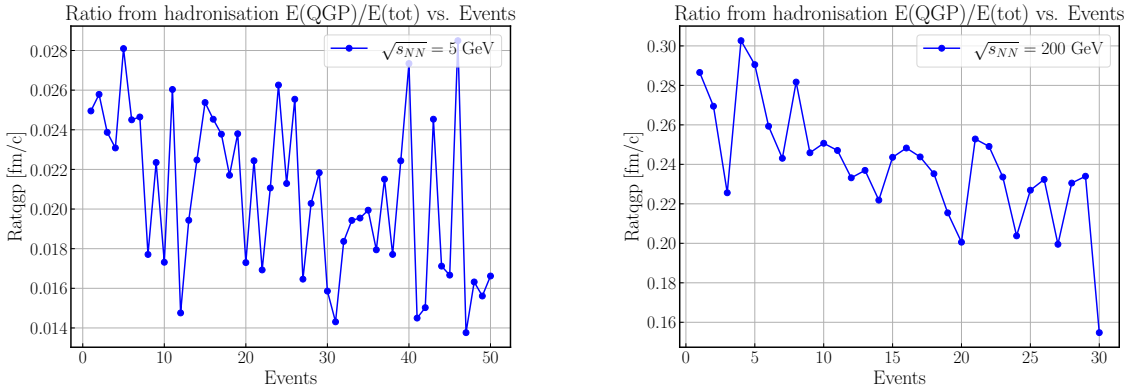

FIG. 4.9: Total QGP energy fraction ratio $R_i[fm/c]$ from the PHSD as a function of time in central (impact parameter $b = 2.2$ fm) Au+Au at $\sqrt{s_{NN}} = 200 - 5$ GeV.

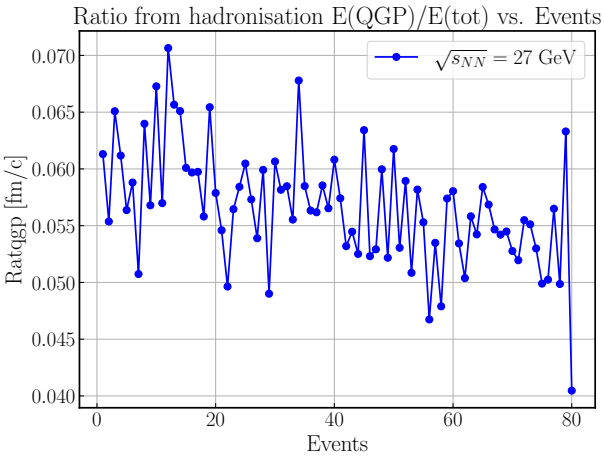

FIG. 4.10: The QGP energy fraction from the PHSD as a function of time in central (impact parameter $b = 2.2$ fm) Au+Au at $\sqrt{s_{NN}} = 27$ GeV.

Chapter 5 Electromagnetic probes

5.1 Dilepton production sources

Dileptons (e^+e^- or $\mu^+\mu^-$ pairs) can be emitted from all stages of the reactions as well as photons. One of the advantages of dileptons - compared to photons - is an additional 'degree of freedom' - the invariant mass M which allows to disentangle various sources:

1. Hadronic sources of dileptons in $p+p, p+A$ and $A+A$ collisions:
   (a) at low invariant masses ($M < 1$ GeV) – the Dalitz decays of mesons and baryons ($\pi^0, \eta, \Delta, ...$) and the direct decay of vector mesons (ρ, ω, ϕ) as well as hadronic bremsstrahlung;
   (b) at intermediate masses ($1 < M < 3$ GeV) – leptons from correlated $D+\bar{D}$ pairs, radiation from multi-meson reactions (π+π, π+ρ, π+ω, ρ+ρ, π+$a_1, ...$) - so called $'4\pi'$ contributions;
   (c) at high invariant masses ($M > 3$ GeV) – the direct decay of vector mesons ($J/\Psi, \Psi'$) and initial 'hard' Drell-Yan annihilation to dileptons (q+$\bar{q} \rightarrow l^+$+l^-, where $l = e, \mu$).
2. 'Thermal' QGP dileptons radiated from the partonic interactions in $A+A$ collisions that contribute dominantly to the intermediate masses. The leading processes are the 'thermal' $q\bar{q}$ annihilation ($q+\bar{q} \rightarrow l^+ + l^-$, $q+\bar{q} \rightarrow g+l^+ + l^-$) and Compton scattering ($q(\bar{q}) + g \rightarrow q(\bar{q}) + l^+ + l^-$).
3. Primary Drell-Yan ($q+\bar{q} \rightarrow l^+ + l^-$) from initial NN collisions

5.2 Dilepton channels in PHSD

The dilepton routines are included in PHSD for simulations of dileptons from $A+A$, $p+A$ as well as from elementary pp and pd reactions. The PHSD can be used also for π^-p and π^-A reactions. It includes also **in-medium effects for vector mesons**, i.e. the dropping mass scenario and collisional broadening. The vector mesons are produced and propagated with their in-medium spectral functions using off-shell dynamics (see Refs. [53, 54, 55, 56, 8]).

The dilepton ($l^+l^- = e^+e^-$ or $\mu^+\mu^-$) spectra are calculated perturbatively with the time integration method. For the details of the dilepton implementation from hadronic channels see our review [20] and also Refs. [57, 56, 38, 58, 59, 60, 61, 62, 63]

The time integration is performed over the actual dilepton emission rate during the full

Table 5.1: Dilepton channels

i	Hadronic dilepton channels: (fort.925)	
1	Dalitz decay of π^0:	$\pi^0 \to \gamma e^+ e^-$
2	Dalitz decay of η:	$\eta \to \gamma l^+ l^-$
3	Dalitz decay of ω:	$\omega \to \pi^0 l^+ l^-$
4	Dalitz decay of Δ:	$\Delta \to N l^+ l^-$
5	Direct decay of ω:	$\omega \to l^+ l^-$
6	Direct decay of ρ:	$\rho \to l^+ l^-$
7	Direct decay of ϕ:	$\phi \to l^+ l^-$
8	Direct decay of J/Ψ:	$J/\Psi \to l^+ l^-$
9	Direct decay of Ψ':	$\Psi' \to l^+ l^-$
10	Dalitz decay of η':	$\eta' \to \gamma l^+ l^-$
11	pn bremsstrahlung:	$pn \to pn l^+ l^-$
12	$\pi^\pm N$ bremsstrahlung:	$\pi^\pm N \to \pi N l^+ l^-$
14	Dalitz decay of a_1:	$a_1 \to \pi l^+ l^-$
15	optional (perturbative N(1520)	$\pi + N \to N(1520) \to l^+ l^- N$
16	optional (perturbative N(1520)	$N + N \to N(1520) \to l^+ l^- N N$
17	primary Drell-Yan	$q\bar{q} \to l^+ l^-$
	QGP dilepton channels: (fort.926)	
18	thermal annihilation	$q\bar{q} \to l^+ l^-$
19	Gluon Bremsstrahlung	$q + \bar{q} \to g + l^+ + l^-$
20	Gluon Compton Scattering	$g + q \to g + l^+ + l^-$
13	sum of ALL hadronic channels	

reaction time (contrary to the 'spontaneous decay' assumption which counts the dilepton radiation only at freeze-out). All branching ratios, electromagnetic partial and total decay widths are taken from the PDG [64].

The pn and $\pi^\pm N$ bremsstrahlung channels are calculated in the soft-photon approximation (SPA). Only elastic pn and $\pi^\pm N$ collisions are accounted in the bremsstrahlung (i.e. $pn \to pne^+e^-$, $\pi^\pm N \to \pi N e^+ e^-$). We stress that the SPA approximation might be considered as an upper limit for the bremsstrahlung contribution (especially for πN). The bremsstrahlung channels are switched off for $E_{\rm lab} \geq 6$ GeV since it is very questionable to use the SPA at high energies.

The channel $\rho \to e^+e^-$ includes the dilepton radiation by all ρ mesons produced in baryon-baryon, meson-baryon or meson-meson (e.g. $\pi^+\pi^-$ annihilation) collisions. The same holds for the other mesons – $\rho, \eta, \omega, \phi, J/\Psi, \Psi'$.

For the implementation of dileptons from QGP channels in the PHSD we refer to the review [8], as well as to Ref. [63] which includes also dileptons from primary Drell-Yann processes and dileptons from QGP including the (T, μ_B) dependence of partonic interactions. The implementation of the dileptons from correlated charm is described in Refs. [65, 63].

5.2.1 Dalitz decays $A \to B\ l^+l^-$

Here l^+l^- are electron e^+e^- or muon $\mu^+\mu^-$ pairs, i.e. $m_l = m_e = 0.511 \cdot 10^{-3}$ GeV or $m_l = m_\mu = 0.105658389$ GeV. For convenience, one can define the quantity:

$$A = \left(1 - 4\frac{m_l^2}{M^2}\right)^{1/2} \left(1 + 2\frac{m_l^2}{M^2}\right) \tag{5.2.1}$$

where M if the mass of the decaying particle.

Dalitz decay $\pi^0 \to \gamma\ l^+l^-$

$$\frac{d\Gamma^{\pi^0\to\gamma\ l+l-}}{dM} = \frac{4\alpha}{3\pi}\frac{\Gamma^{\pi^0\to\gamma\gamma}}{M}|F^{\pi^0\to\gamma\gamma}(M)|^2 A \left(1 - \frac{M^2}{m_\pi^2}\right)^3, \tag{5.2.2}$$

where

$$\begin{cases} F^{\pi^0\to\gamma\gamma}(M) = 1 + B_{\pi^0} M^2, \\ \qquad\qquad \text{with } B_{\pi^0} = 5.5 \text{ GeV}^{-2}, \\ \Gamma^{\pi^0\to\gamma\gamma} = 7.8 \cdot 10^{-9} \text{ GeV}, \\ \Gamma^{\pi^0}_{\text{tot}} \simeq \Gamma^{\pi^0\to\gamma\gamma}, \\ Br^{\pi^0\to\gamma\gamma} = 0.988. \end{cases} \tag{5.2.3}$$

Dalitz decay $\eta \to \gamma\ l^+l^-$

$$\frac{d\Gamma^{\eta\to\gamma\ l+l-}}{dM} = \frac{4\alpha}{3\pi}\frac{\Gamma^{\eta\to\gamma\gamma}}{M}|F^{\eta\to\gamma\gamma}(M)|^2 A \left(1 - \frac{M^2}{m_\eta^2}\right)^3, \tag{5.2.4}$$

where

$$\begin{cases} F^{\eta\to\gamma\gamma}(M) = \left(1 - \frac{M^2}{\Lambda_\eta^2}\right)^{-1}, \\ \qquad\qquad \text{with } \Lambda_\eta = 0.72 \text{ GeV}, \\ \Gamma^{\eta\to\gamma\gamma} = 4.6 \cdot 10^{-7} \text{ GeV}, \\ \Gamma^{\eta}_{\text{tot}} = 1.18 \cdot 10^{-6} \text{ GeV}, \\ Br^{\eta\to\gamma\gamma} = 0.3933. \end{cases} \tag{5.2.5}$$

Dalitz decay $\omega \to \gamma\ l^+l^-$

$$\begin{aligned} \frac{d\Gamma^{\omega\to\pi^0\ l+l-}}{dM} =& \frac{2\alpha}{3\pi}\frac{\Gamma^{\omega\to\pi^0\gamma}}{M}|F^{\omega\to\pi^0\gamma}(M)|^2 A \\ & \left[\left(1 + \frac{M^2}{(m_\omega^2 - m_\pi^2)}\right)^2 - \frac{4m_\omega^2 M^2}{(m_\omega^2 - m_\pi^2)^2}\right]^{3/2}, \end{aligned} \tag{5.2.6}$$

where

$$\begin{cases} |F^{\omega\to\pi^0\gamma}(M)|^2 = \frac{\Lambda_\omega^4}{(\Lambda_\omega^2-M^2)^2+\Lambda_\omega^2\Gamma_\omega^2}, \\ \quad \text{with } \Lambda_\omega = 0.65 \text{ GeV}, \\ \quad \text{and } \Gamma_\omega = 0.075 \text{ GeV}, \\ \Gamma^{\omega\to\pi^0\gamma} = 7.17\cdot 10^{-4} \text{ GeV}, \\ \Gamma^{\omega}_{\text{tot}} = 8.44\cdot 10^{-3} \text{ GeV}, \\ Br^{\omega\to\pi^0\gamma} = 0.085 \end{cases} \tag{5.2.7}$$

Dalitz decay $\eta' \to \gamma\ l^+l^-$

$$\frac{d\Gamma^{\eta'\to\gamma\ l+l-}}{dM} = \frac{4\alpha}{3\pi}\frac{\Gamma^{\eta'\to\gamma\gamma}}{M}|F^{\eta'\to\gamma\gamma}(M)|^2 A\left(1-\frac{M^2}{m_{\eta'}^2}\right)^3, \tag{5.2.8}$$

where

$$\begin{cases} |F^{\eta'\to\gamma\gamma}(M)|^2 = \frac{\Lambda_{\eta'}^4}{(\Lambda_{\eta'}^2-M^2)^2+\Lambda_{\eta'}^2\Gamma_{\eta'}^2}, \\ \quad \text{with } \Lambda_{\eta'} = 0.75 \text{ GeV}, \\ \quad \text{and } \Gamma_{\eta'} = 0.14 \text{ GeV}, \\ \Gamma^{\eta'\to\gamma\gamma} = 4.28\cdot 10^{-6} \text{ GeV}, \\ \Gamma^{\eta'}_{tot} = 0.202\cdot 10^{-3} \text{ GeV}, \\ Br^{\eta'\to\gamma\gamma} = 0.0212 \\ m_{\eta'} = 0.95778 \text{ GeV}. \end{cases} \tag{5.2.9}$$

Dalitz decay $\Delta \to N\ l^+l^-$

$$\frac{d\Gamma^{\Delta\to N\ l+l-}}{dM} = \frac{2\alpha}{3\pi}\frac{\Gamma_0(M,M_\Delta)}{M}, \tag{5.2.10}$$

with

$$\Gamma_0(M,M_\Delta) = \frac{\lambda^{1/2}(M^2,m_N^2,M_\Delta^2)}{16\pi M_\Delta^2}\cdot m_N\cdot[2m_T(M,M_\Delta)+m_L(M,M_\Delta)], \tag{5.2.11}$$

and

$$\begin{aligned} m_L(M,M_\Delta) =& (efg)^2\frac{M_\Delta^2}{9m_N}M^2\cdot 4(M_\Delta-m_N-q_0), \\ m_T(M,M_\Delta) =& (efg)^2\frac{M_\Delta^2}{9m_N}\left[q_0^2(5M_\Delta-3(q_0+m_N))-M^2(M_\Delta+m_N+q_0)\right] \end{aligned} \tag{5.2.12}$$

where

$$\begin{cases} \lambda(M^2, m_N^2, M_\Delta^2) = M^4 + m_N^4 + M_\Delta^4 \\ \qquad\qquad -2(M^2 m_N^2 + M^2 M_\Delta^2 + m_N^2 M_\Delta^2), \\ e^2 = 4\pi\alpha, \\ f = -1.5 \frac{M_\Delta + m_N}{m_N((m_N+M_\Delta)^2 - M^2)}, \\ g = 5.44, \\ q_0 = \sqrt{M^2 + p_f^2}, \\ p_f^2 = (M_\Delta^2 - (m_N + M)^2)(M_\Delta^2 - (m_N - M)^2)/4M_\Delta^2. \end{cases} \tag{5.2.13}$$

Here M_Δ is the current mass of the Δ-resonance, calculated according to the spectral function with the total width from Ref. [66] (cf. also Ref. [67]):

$$\Gamma_{tot}^{\Delta}(M_\Delta) = \Gamma_R \frac{M_{\Delta 0}}{M_\Delta} \cdot \left(\frac{q}{q_r}\right)^3 \cdot F^2(q), \tag{5.2.14}$$

where

$$\begin{cases} F(q) = \frac{\beta_r^2 + q_r^2}{\beta^2 + q^2}, \\ q^2 = (M_\Delta^2 - (m_N + m_\pi)^2)(M_\Delta^2 - (m_N - m_\pi)^2)/4M_\Delta^2, \\ q_r^2 = 0.051936, \\ \beta_r^2 = 0.09, \\ \Gamma_R = 0.11 \text{ GeV}, \\ M_{\Delta 0} = 1.232 \text{ GeV}. \end{cases} \tag{5.2.15}$$

5.2.2 Direct decay of vector mesons $V \to l^+l^-$

The dilepton decay width of vector meson V with the mass M (calculated in PHSD according to the spectral function) is

$$\Gamma^{V\to l^+l^-}(M) = C\frac{m_V^4}{M^3}, \tag{5.2.16}$$

where $C = \frac{\Gamma^{V\to l^+l^-}(m_V)}{m_V}$, m_V is the pole mass of the vector meson V.

For broad resonances such as the ρ meson, the branching ratio to dileptons depends on the mass M:

$$Br^{V\to l^+l^-}(M) = \frac{\Gamma^{V\to l^+l^-}(M)}{\Gamma_{\text{tot}}^V(M)}. \tag{5.2.17}$$

Here the total width of the ρ meson is

$$\Gamma_{\text{tot}}^{\rho}(M) \simeq \Gamma_{\rho\to\pi\pi} = \Gamma_0 \left(\frac{m_V}{M}\right)^2 \left(\frac{q}{q_V}\right)^3, \tag{5.2.18}$$

with

$$\begin{cases} q = (M^2 - 4m_\pi^2)^{1/2}/2, \\ q_V = (m_V^2 - 4m_\pi^2)^{1/2}/2. \end{cases} \tag{5.2.19}$$

For narrow resonances such as $\omega, \phi, J/\Psi, \Psi'$ a constant total width and branching ratio are used: $\Gamma_{\text{tot}}^V \equiv \Gamma_{\text{tot}}(m_V)$, $Br_0^{V\to l^+l^-} \equiv Br^{V\to l^+l^-}(m_V)$.

Table 5.2: The parameters for dilepton decay of vector mesons.

mesons	$\to e^+e^-$	$\to \mu^+\mu^-$
ρ	$Br = 4.49 \cdot 10^{-5}$ $\Gamma = 6.77 \cdot 10^{-6}$ GeV $C = 8.814 \cdot 10^{-6}$	$Br = 4.6 \cdot 10^{-5}$ $\Gamma = 6.9 \cdot 10^{-6}$ GeV $C = 8.96 \cdot 10^{-6}$
ω	$Br = 7.07 \cdot 10^{-5}$ $\Gamma = 0.6 \cdot 10^{-6}$ GeV $C = 0.767 \cdot 10^{-6}$	$Br = 8.06 \cdot 10^{-5}$ $\Gamma = 0.68 \cdot 10^{-6}$ GeV $C = 0.863 \cdot 10^{-6}$
ϕ	$Br = 2.91 \cdot 10^{-4}$ $\Gamma = 1.297 \cdot 10^{-6}$ GeV $C = 1.27 \cdot 10^{-6}$	$Br = 3.7 \cdot 10^{-4}$ $\Gamma = 1.649 \cdot 10^{-6}$ GeV $C = 1.618 \cdot 10^{-6}$
J/Ψ	$Br = 5.93 \cdot 10^{-2}$ $\Gamma = 5.26 \cdot 10^{-6}$ GeV $C = 1.698 \cdot 10^{-6}$	$Br = 5.88 \cdot 10^{-2}$ $\Gamma = 5.12 \cdot 10^{-6}$ GeV $C = 1.652 \cdot 10^{-6}$
Ψ'	$Br = 8.8 \cdot 10^{-3}$ $\Gamma = 2.12 \cdot 10^{-6}$ GeV $C = 0.575 \cdot 10^{-6}$	$Br = 1.03 \cdot 10^{-2}$ $\Gamma = 2.853 \cdot 10^{-6}$ GeV $C = 0.774 \cdot 10^{-6}$

5.2.3 Activation of dileptons in the *inputPHSD* file

In order to activate the calculation of dilepton yields in the PHSD the user has to activate the following flags in *inputPHSD* as:

IDILEPT - flag to activate perturbative dileptons:
IDILEPT=0 - without dileptons,
IDILEPT=1 - electron pairs (e^+e^-),
IDILEPT=2 - muon pairs ($\mu^+\mu^-$)

ICQ - flag to activate the in-medium effects for vector mesons:
ICQ=0 - without in-medium effects (free spectral functions),
ICQ=1 - dropping mass scenario,
ICQ=2 - collisional broadening

The calculations of primary Drell-Yan, can be activated by setting flag *InitialDY=1* in ini_param.f.

5.2.4 Output files for dilepton yields: *fort.925* and *fort.926*

If IDILEPT=1, the multi-differential dilepton yields (multiplicity) $\frac{dN_i}{dM dp_T dy}$ are calculated dynamically using the time integration method for each impact parameter b for all dilepton channels i from Table 5.1.

There are 2 output files for dilepton yields:

fort.925 - from hadronic channels $i = 1 - 12, 14$
- from primary Drell-Yann $i = 17$

fort.926 - from partonic (QGP) channels $i = 18 - 20$. This file is created if the QGP is activated by flag IGLUE=1 in *inputPHSD*.

Output file *fort.925* and *fort.926* - final dileptons

b [fm]

M [GeV]	y	p_T [GeV]	$\frac{dN_i(b)}{dMdp_Tdy}$ [GeV^{-2}] for $i = 1, 2, ..., 17$
...	...	...	...
M_1	y_1	p_{T1}	...
M_1	y_1	p_{T2}	...
...	...	...	...
M_1	y_1	$p_{TN_{p_T}}$	...
M_1	y_2	p_{T1}	...
M_1	y_2	p_{T2}	...
...	...	...	...
M_1	y_2	$p_{TN_{p_T}}$	...
...	...	...	...
M_1	y_{N_y}	p_{T1}	...
M_1	y_{N_y}	p_{T2}	...
...	...	...	...
M_1	y_{N_y}	$p_{TN_{p_T}}$	...
...	...	...	...
M_{N_M}	y_{N_y}	p_{T1}	...
M_{N_M}	y_{N_y}	p_{T2}	...
...	...	...	...
M_{N_M}	y_{N_y}	$p_{TN_{p_T}}$	...

- b is the impact parameter in fm
- M is the invariant mass of dileptons in GeV.
  The grid is defined in the dilepton routine *diltimeint* in *dilepton.f* as: $M_J = \Delta_M \cdot j,\ j = 1, ..., N_M,\ \Delta_M = 0.01$ is the step in invariant mass in GeV; the number of steps $N_M = 400$ for CBM, SPS, RHIC, LHC and $N_M = 200$ for HADES.
- y is the dilepton rapidity in the calculational frame (e.g. in the center-of-mass system for $A + A$).
  The grid in y: $-\Delta_y \cdot N_y \leq y \leq \Delta_y \cdot N_y$, $\Delta_y = 0.2$ is the step in y, $N_y = 25$.
- p_T is the dilepton transverse momentum in GeV/c.
  The grid in p_T: $p_{Tj} = \Delta_{p_T} \cdot k,\ k = 1, ..., N_{p_T},\ \Delta_{p_T} = 0.1$ is the step in p_T, $N_{p_T} = 50$.
- $dN_i(b)/dMdp_Tdy$ is the differential dilepton multiplicity for individual channels $i = 1, 2, ..., N, N + 1$ from Table 4. Presently there are 12 channels ($N = 12$), the last column corresponds to the sum over all channels ($N + 1 = 13$).
  Here $dN_i(b)/dMdp_Tdy$ is avaraged over the number of subsequent runs (ISUBS) and parallel events (NUM) for each impact parameter b (cf. Eq. (2)).
  New: $\pi^{\pm}N$ bremsstrahlung (N=12) is excluded from the sum over all channels

(N=13), however, it is still written out in file *fort.925*.

We DO NOT recommend to reconstruct the dilepton yield per each INDIVIDUAL event (e.g. each $A+A$ collision) since the statistical fluctuations in the dilepton spectra per event are large. In our opinion it is more reasonable to consider that in each physical event (for given b) the dilepton production is the same, so the final yield for one event corresponds to the "average" over manyevents (ISUBS and NUM).

Using the differential dilepton yield $dN_i(b)/dMdp_Tdy$ one can calculate the differential dilepton cross section or yield. This procedure depends on IBweight_MC.

If IBweight_MC=0, the dilepton observables are calculated by integration over the impact parameter (similar to hadronic observables):

$$\begin{aligned} \frac{d\sigma_i}{dMdp_Tdy}\left[\frac{\text{mb}}{\text{GeV}^2}\right] &= 10\int_{b_{min}}^{b_{max}} db\ 2\pi\ b\ \frac{dN_i(b)}{dMdp_Tdy} \\ &\Rightarrow 10\sum_{b_{min}}^{b_{max}} \Delta b\ 2\pi\ b\ \frac{dN_i(b)}{dMdp_Tdy}. \end{aligned} \tag{5.2.20}$$

If IBweight_MC=1, one needs just to sum the multiple output from different PHSD "jobs" for each (M, y, p_T) bin and then integrate over corresponding variables, e.g. over dy, dp_T to obtain dN/dM spectra.

Also by integrating over M, y or p_T one can obtain the dilepton mass spectra (cross section or multiplicity) dN/dp_T, rapidity distribution dN/dy or p_T distribution dN/dp_T.

5.2.5 Analysis program for dileptons

dileptons_PHSD_PHQMD.f

That is an example program to calculate dilepton invariant mass, transverse momentum, rapidity, and transverse mass spectra using the generated dilepton output files for $A+A$, $p+A$, $p+p$, $\pi+A$, and $\pi+p$. Additionally, experimental cuts/acceptances from STAR/ALICE/HADES can be applied.

Input files:

- inputPHSD (initial setup of the collision and initial parameters);
- fort.925 (List of hadronic channels);
- fort.926 (List of partonic channels);

Output files:

- dndm.dat (invariant-mass spectra of all dilepton channels);
- dndpt.dat (transverse momentum spectra of all dilepton channels);
- dndy.dat (rapidity spectra of all dilepton channels);

Furthermore, the file 'dileptons_PHSD_PHQMD.f' contains a list of initial parameters for the analysis:

iflag This flag selects whether the routine calculates dilepton yields or differential cross sections. If `iflag = 1` (by default), the code computes the dilepton multiplicity (yield), for example dN/dM in units of 1/GeV. If `iflag = 2`, the code computes the dilepton differential cross section, for example $d\sigma/dM$ in units of mb/GeV.

IACCtype This flag selects the detector acceptance or kinematic filter applied during the analysis. The available options are:

- `IACCtype = 1`: STAR acceptance,
- `IACCtype = 2`: HADES acceptance,
- `IACCtype = 3`: ALICE acceptance,
- `IACCtype = 4`: no acceptance filter (by default),
- `IACCtype = 5`: pseudorapidity cut $|\eta| < 1$.

Inormpi0 This flag controls whether the output is additionally normalized to the π^0 multiplicity. If `Inormpi0 = 0` (by default), only the standard spectra are written. If `Inormpi0 = 1`, the routine prints output files normalized to the pion yield, such as:

• dndm_pi0.dat (invariant-mass spectra of all dilepton channels normalized to the π^0 multiplicity);
• dndpt_pi0.dat (transverse momentum spectra of all dilepton channels normalized to the π^0 multiplicity);
• dndy_pi0.dat (rapidity spectra of all dilepton channels normalized to the π^0 multiplicity);

IMbincal This flag controls whether additional spectra are printed for selected invariant-mass intervals. If `IMbincal = 1`, the routine generates dN/dp_T and dN/dy for the following mass bins: $M_1 < 0.15$ GeV, $0.15 \leq M_2 < 0.55$ GeV, and $M_3 \geq 0.55$ GeV, generating the output:

• dndpt_M1.dat (transverse momentum spectra of all dilepton channels for the mass bin: $M_1 < 0.15$ GeV);
• dndpt_M2.dat (transverse momentum spectra of all dilepton channels for the mass bin: $0.15 \leq M_2 < 0.55$ GeV);
• dndpt_M3.dat (transverse momentum spectra of all dilepton channels for the mass bin: $M_3 \geq 0.55$ GeV);

Additional output options

Several optional flags enable the production of extra output files and integrated observables.

IQGPout This flag enables a separate output file for the QGP contribution. If `IQGPout = 1`, the code writes the file:

• QGP_sum.dat (invariant-mass spectra of the individual QGP channels and their sum);

IDYout This flag enables a separate output file for the initial Drell–Yan contribution. If `IDYout = 1`, the code writes the file:

• initial_DY.dat (invariant-mass spectra of the initial Drell-Yann);

dilExcess This flag enables the calculation of the dilepton excess yield in the intermediate low-mass region. If `dilExcess = 1`, the routine evaluates the dilepton excess in the interval $0.4 < M < 0.75$ GeV, including the contributions from Δ, a_1, ρ, and QGP channels (for more details see Refs. [63, 68]).

• dilep_excess.dat (invariant-mass spectra of the dilepton excess yield in the intermediate low-mass region.);

dilyield_imr This flag enables the calculation of the dilepton yield in the intermediate-mass region. If `dilyield_imr = 1`, the routine evaluates the dilepton yield in the interval $1.2 < M < 3.0$ GeV, including the initial Drell–Yan and QGP contributions (for more details see Refs. [63, 65]).

• dilep_yield_QGP.dat (invariant-mass spectra of the dilepton yield in the intermediate-mass region);

The program includes `subroutine simulate_ee(...)` allows to simulate e^+e^- or $\mu^+\mu^-$ pairs for given impact parameter b using the calculated differential dilepton spectra $dN_i(b)/dMdp_Tdy$ from *fort.925*. The idea is to simulate dilepton pairs – as many as one needs, i.e. N_{ee} for each bin in the grid (M, y, p_T) and for each dilepton channel $i = 1, .., N$ – in order to propagate it later on through the detector system (or employ the experimental filter). The 'weight' for each dilepton pair (and single e^+ or e^-) which passed the acceptance is $dN_i(b)/dMdp_Tdy \cdot 1/N_{ee}$.

Figure 5.1 shows the PHSD result [63] for the dilepton invariant mass spectra for Au+Au collisions for $0 - 80\%$ centrality at $\sqrt{s_{NN}} = 200$ GeV in comparison to STAR data [69].

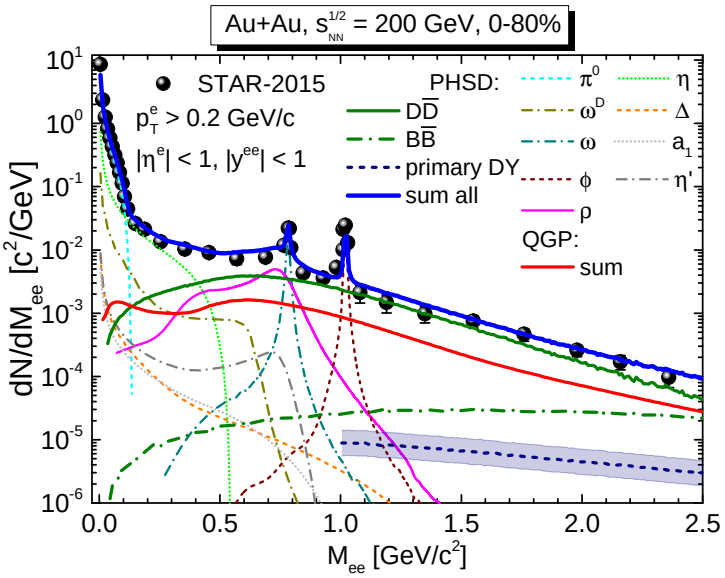

FIG. 5.1: Invariant mass spectra of dileptons from PHSD [63] in comparison to STAR data for Au+Au collisions for $0-80\%$ centrality at $\sqrt{s_{NN}} = 200$ GeV [69]. The total yield is shown by the blue lines while the different contributions are specified in the legends. The solid dots represent the STAR data. The theoretical calculations are passed through the corresponding STAR acceptance filter and mass/momentum resolution.

5.3 Photons

The inclusive photon production from p + p, p + A and A + A collisions - divided into 'decay photons' and 'direct photons' - have been studies within the PHSD in a past. For the details we refer to the Ref. [8] and references there.

Chapter 6 Heavy flavors

6.1 Charm/bottom quark dynamics

The charm/bottom dynamics in the PHSD is described in Refs. [70, 71, 65, 72].

6.2 Open/hidden heavy flavors

In order to activate the dynamics of heavy flavors, set the flag `IHARD` = 1 in *inputPHSD*. This flag activates the correct heavy flavor initial production according to binary NN collisions as well as a heavy quark dynamics in the QGP phase and the final hadronic interactions.

Note, if one runs the code with `IHARD` = 0, the charm/bottom hadrons will still show up in *phsd.dat* since they come from PYTHIA fragmentation, however, they should NOT be used for the study charm/bottom physics. However, if you are NOT interested in heavy flavor physics, we recommend to set `IHARD` = 0 to speed up the calculations, noting that charm/bottom only very slightly affect the 'bulk' dynamics.

The list of open and hidden charm/bottom mesons/baryons in the PHSD is indicated in Tables 1.6, 1.7 and 1.8 as well as charm/bottom baryons in Tables 1.3 and 1.4.

The final charm/bottom hadrons are written in output files *phsd.dat* together with other hadrons.

Bibliography

[1] W. Cassing and E. L. Bratkovskaya. Parton transport and hadronization from the dynamical quasiparticle point of view. *Phys. Rev. C*, 78:034919, 2008.

[2] W. Cassing. From Kadanoff-Baym dynamics to off-shell parton transport. *Eur. Phys. J. ST*, 168:3–87, 2009.

[3] Pierre Moreau, Olga Soloveva, Lucia Oliva, Taesoo Song, Wolfgang Cassing, and Elena Bratkovskaya. *Exploring the partonic phase at finite chemical potential within an extended off-shell transport approach.* Phys. Rev. C **100** (2019) 014911.

[4] J. Aichelin, E. Bratkovskaya, A. Le Fèvre, V. Kireyeu, V. Kolesnikov, Y. Leifels, V. Voronyuk, and G. Coci. Parton-hadron-quantum-molecular dynamics: A novel microscopic n -body transport approach for heavy-ion collisions, dynamical cluster formation, and hypernuclei production. *Phys. Rev. C*, 101(4):044905, 2020.

[5] Gabriele Coci, Susanne Gläßel, Viktar Kireyeu, Jörg Aichelin, Christoph Blume, Elena Bratkovskaya, Vadim Kolesnikov, and Vadim Voronyuk. Dynamical mechanisms for deuteron production at mid-rapidity in relativistic heavy-ion collisions from energies available at the GSI Schwerionensynchrotron to those at the BNL Relativistic Heavy Ion Collider. *Phys. Rev. C*, 108(1):014902, 2023.

[6] W. Cassing and E. L. Bratkovskaya. Parton-Hadron-String Dynamics: an off-shell transport approach for relativistic energies. *Nucl. Phys.*, A831:215–242, 2009.

[7] E. L. Bratkovskaya, W. Cassing, V. P. Konchakovski, and O. Linnyk. Parton-Hadron-String Dynamics at Relativistic Collider Energies. *Nucl. Phys.*, A856:162–182, 2011.

[8] O. Linnyk, E. L. Bratkovskaya, and W. Cassing. Effective QCD and transport description of dilepton and photon production in heavy-ion collisions and elementary processes. *Prog. Part. Nucl. Phys.*, 87:50–115, 2016.

[9] L. P. Kadanoff and G. Baym. *Quantum Statistical mechanics.* W. A. Benjamin, Inc., New York, 1962.

[10] S. Juchem, W. Cassing, and C. Greiner. Nonequilibrium quantum field dynamics and off-shell transport for phi**4 theory in (2+1)-dimensions. *Nucl. Phys.*, A743:92–126, 2004.

[11] W. Cassing. Dynamical quasiparticles properties and effective interactions in the sQGP. *Nucl. Phys.*, A795:70–97, 2007.

[12] W. Cassing. QCD thermodynamics and confinement from a dynamical quasiparticle point of view. *Nucl. Phys.*, A791:365–381, 2007.

[13] Y. Aoki, Szabolcs Borsanyi, Stephan Durr, Zoltan Fodor, Sandor D. Katz, Stefan Krieg, and Kalman K. Szabo. The QCD transition temperature: results with physical masses in the continuum limit II. *JHEP*, 06:088, 2009.

[14] M. Cheng et al. The QCD equation of state with almost physical quark masses. *Phys. Rev.*, D77:014511, 2008.

[15] W. Cassing, O. Linnyk, T. Steinert, and V. Ozvenchuk. Electrical Conductivity of Hot QCD Matter. *Phys. Rev. Lett.*, 110(18):182301, 2013.

[16] Olga Soloveva, Pierre Moreau, and Elena Bratkovskaya. Transport coefficients for the hot quark-gluon plasma at finite chemical potential μ_B. *Phys. Rev. C*, 101(4):045203, 2020.

[17] Jan A. Fotakis, Olga Soloveva, Carsten Greiner, Olaf Kaczmarek, and Elena Bratkovskaya. Diffusion coefficient matrix of the strongly interacting quark-gluon plasma. *Phys. Rev. D*, 104(3):034014, 2021.

[18] Ilia Grishmanovskii, Taesoo Song, Carsten Greiner, and Elena Bratkovskaya. Transport coefficients of heavy quarks by elastic and radiative scatterings in the strongly interacting quark-gluon plasma. *Phys. Rev. D*, 112(1):014042, 2025.

[19] W. Ehehalt and W. Cassing. *Relativistic transport approach for nucleus-nucleus collisions from SIS to SPS energies*. Nucl. Phys. A **602** (1996) 449–486.

[20] W. Cassing and E. L. Bratkovskaya. *Hadronic and electromagnetic probes of hot and dense nuclear matter*. Phys. Rep. **308** (1999) 65–233.

[21] Bo Andersson, G. Gustafson, and Hong Pi. The FRITIOF model for very high-energy hadronic collisions. *Z. Phys.*, C57:485–494, 1993.

[22] W. Cassing, L. Tolos, E. L. Bratkovskaya, and A. Ramos. Anti-kaon production in A+A collisions at SIS energies within an off-shell G matrix approach. *Nucl. Phys.*, A727:59–94, 2003.

[23] Susanne Gläßel, Viktar Kireyeu, Vadim Voronyuk, Jörg Aichelin, Christoph Blume, Elena Bratkovskaya, Gabriele Coci, Vadim Kolesnikov, and Michael Winn. Cluster and hypercluster production in relativistic heavy-ion collisions within the parton-hadron-quantum-molecular-dynamics approach. *Phys. Rev. C*, 105(1):014908, 2022.

[24] Viktar Kireyeu, Jan Steinheimer, Jörg Aichelin, Marcus Bleicher, and Elena Bratkovskaya. Deuteron production in ultrarelativistic heavy-ion collisions: A comparison of the coalescence and the minimum spanning tree procedure. *Phys. Rev. C*, 105(4):044909, 2022.

[25] V. Kireyeu, G. Coci, S. Glaessel, J. Aichelin, C. Blume, and E. Bratkovskaya. Cluster formation near midrapidity: How the production mechanisms can be identified experimentally. *Phys. Rev. C*, 109(4):044906, 2024.

[26] J. Aichelin. 'Quantum' molecular dynamics: A Dynamical microscopic n body approach to investigate fragment formation and the nuclear equation of state in heavy ion collisions. *Phys. Rept.*, 202:233–360, 1991.

[27] J. Aichelin, A. Rosenhauer, G. Peilert, Horst Stoecker, and W. Greiner. Importance of Momentum Dependent Interactions for the Extraction of the Nuclear Equation of State From High-energy Heavy Ion Collisions. *Phys. Rev. Lett.*, 58:1926–1929, 1987.

[28] J. Aichelin, A. Bohnet, G. Peilert, Horst Stoecker, W. Greiner, and A. Rosenhauer. Quantum Molecular Dynamics Approach to Heavy Ion Collisions: Description of the Model, Comparison With Fragmentation Data, and the Mechanism of Fragment Formation. *Phys. Rev. C*, 37:2451–2468, 1988.

[29] C. Hartnack, Rajeev K. Puri, J. Aichelin, J. Konopka, S. A. Bass, Horst Stoecker, and W. Greiner. Modeling the many body dynamics of heavy ion collisions: Present status and future perspective. *Eur. Phys. J. A*, 1:151–169, 1998.

[30] Viktar Kireyeu, Vadim Voronyuk, Michael Winn, Susanne Gläßel, Jörg Aichelin, Christoph Blume, Elena Bratkovskaya, Gabriele Coci, and Jiaxing Zhao. Constraints on the equation-of-state from low energy heavy-ion collisions within the PHQMD microscopic approach with momentum-dependent potential. 11 2024.

[31] Yingjie Zhou et al. Probing the nuclear equation of state with clusters and hypernuclei. *Phys. Rev. C*, 113(1):014909, 2026.

[32] L. A. Kondratyuk, M. Krivoruchenko, N. Bianchi, E. De Sanctis, and V. Muccifora. *Suppression of nucleon resonances in the total photoabsorption on nuclei*. Nucl. Phys. A **579** (1994) 453.

[33] R. Rapp and J. Wambach. *Chiral symmetry restoration and dileptons in relativistic heavy ion collisions*. Adv. Nucl. Phys. **25** (2000) 1.

[34] L. Tolós, A. Ramos, and A. Polls. *Antikaon nuclear potential in hot and dense matter*. Phys. Rev. C **65** (2002) 054907.

[35] N. Bianchi et al. *Absolute measurement of the total photoabsorption cross section for carbon in the nucleon resonance region*. Phys. Lett. B **309** (1993) 5.

[36] N. Bianchi et al. *Absolute total photoabsorption cross sections on nuclei in the nucleon resonance region*. Phys. Lett. B **325** (1994) 333.

[37] N. Bianchi et al. *Total hadronic photoabsorption cross section on nuclei in the nucleon resonance region*. Phys. Lett. B **309** (1993) 5.

[38] E. L. Bratkovskaya, W. Cassing, and U. Mosel. *Perspectives of e^+e^- production in pp, pd and pBe reactions at SIS energies*. Nucl. Phys. A **686** (2001) 568.

[39] M. L. Miller, K. Reygers, S. J. Sanders, and P. Steinberg. Glauber modeling in high energy nuclear collisions. Ann. Rev. Nucl. Part. Sci. **57** (2007) 205.

[40] V. Ozvenchuk, O. Linnyk, M. I. Gorenstein, E. L. Bratkovskaya, and W. Cassing. *Dynamical equilibration of strongly interacting "infinite" parton matter within the parton-hadron-string dynamics transport approach.* Phys. Rev. C **87** (2013) 024901.

[41] W. Cassing and S. Juchem. Semiclassical transport of particles with dynamical spectral functions. *Nucl. Phys. A*, 665:377–400, 2000.

[42] W. Cassing and S. Juchem. Semiclassical transport of hadrons with dynamical spectral functions in A + A collisions at SIS / AGS energies. *Nucl. Phys. A*, 672:417–445, 2000.

[43] Wolfgang Cassing. *Transport Theories for Strongly-Interacting Systems.* Springer Nature: Lecture Notes in Physics 989, 2021.

[44] W. Ehehalt and W. Cassing. Relativistic transport approach for nucleus nucleus collisions from SIS to SPS energies. *Nucl. Phys.*, A602:449–486, 1996.

[45] W. Cassing and E. L. Bratkovskaya. Hadronic and electromagnetic probes of hot and dense nuclear matter. *Phys. Rept.*, 308:65–233, 1999.

[46] A Raab. *Chem. Phys. Lett.*, 319:674, 2000.

[47] J. Broeckhove, L. Lathouwers, E. Kesteloot, and P. Van Leuven. On the equivalence of time-dependent variational principles. *Chemical Physics Letters*, 149(5):547–550, 1988.

[48] H. Feldmeier. FERMIONIC MOLECULAR DYNAMICS. *Nucl. Phys. A*, 515:147–172, 1990.

[49] Akira Ono, Hisashi Horiuchi, Toshiki Maruyama, and Akira Ohnishi. Antisymmetrized version of molecular dynamics with two nucleon collisions and its application to heavy ion reactions. *Prog. Theor. Phys.*, 87:1185–1206, 1992.

[50] S. Hama, B. C. Clark, E. D. Cooper, H. S. Sherif, and R. L. Mercer. Global Dirac optical potentials for elastic proton scattering from heavy nuclei. *Phys. Rev. C*, 41:2737–2755, 1990.

[51] Pierre Moreau, Olga Soloveva, Ilia Grishmanovskii, Vadim Voronyuk, Lucia Oliva, Taesoo Song, Viktar Kireyeu, Gabriele Coci, and Elena Bratkovskaya. Properties of the quark-gluon plasma created in heavy-ion collisions. *Astron. Nachr.*, 342(5):715–726, 2021.

[52] Radoslaw Ryblewski and Wojciech Florkowski. *Highly-anisotropic hydrodynamics in 3+1 space-time dimensions.* Phys. Rev. C **85** (2012) 064901.

[53] W. Cassing and S. Juchem. *Semiclassical transport of particles with dynamical spectral functions.* Nucl. Phys. A **665** (2000) 377.

[54] W. Cassing and S. Juchem. *Semiclassical transport of hadrons with dynamical spectral functions in $A + A$ collisions at SIS/AGS energies.* Nucl. Phys. A **672** (2000) 417.

[55] W. Cassing and S. Juchem. *Equilibration within a semiclassical off-shell transport approach.* Nucl. Phys. A **677** (2000) 445.

[56] E. L. Bratkovskaya. *e^+e^- production in pA reactions at SIS energies.* Nucl. Phys. A **696** (2001) 761.

[57] E. L. Bratkovskaya. *ρ/ω properties from dilepton spectra in pA reactions at 12 GeV.* Phys. Lett. B **529** (2002) 26.

[58] E. L. Bratkovskaya, W. Cassing, M. Effenberger, and U. Mosel. *e^+e^- production from pp reactions at BEVALAC energies.* Nucl. Phys. A **653** (1999) 301.

[59] E. L. Bratkovskaya and C. M. Ko. *Low-mass dileptons and dropping rho meson mass.* Phys. Lett. B **445** (1999) 265.

[60] E. L. Bratkovskaya, W. Cassing, R. Rapp, and J. Wambach. *Dilepton production and m_T-scaling at BEVALAC/SIS energies.* Nucl. Phys. A **634** (1998) 168.

[61] W. Cassing, E. L. Bratkovskaya, R. Rapp, and J. Wambach. *Probing the ρ spectral function in hot and dense nuclear matter by dileptons.* Phys. Rev. C **57** (1998) 916.

[62] E. L. Bratkovskaya and W. Cassing. *Dilepton Production from AGS to SPS Energies within a Relativistic Transport Approach.* Nucl. Phys. A **619** (1997) 413.

[63] Adrian William Romero Jorge, Taesoo Song, Qi Zhou, and Elena Bratkovskaya. Electromagnetic emission from strongly interacting hadronic and partonic matter created in heavy-ion collisions. *Phys. Rev. C*, 111(6):064904, 2025.

[64] J. Beringer et al. *Review of Particle Physics.* Phys. Rev. D **86** (2012) 010001.

[65] Taesoo Song, Wolfgang Cassing, Pierre Moreau, and Elena Bratkovskaya. Open charm and dileptons from relativistic heavy-ion collisions. *Phys. Rev. C*, 97(6):064907, 2018.

[66] J. H. Koch, E. J. Moniz, and N. Ohtsuka. *Nuclear photoabsorption and Compton scattering at intermediate energy.* Ann. Phys. **154** (1984) 99.

[67] Gy. Wolf, G. Batko, W. Cassing, U. Mosel, K. Niita, and M. Schäfer. *Dilepton production in heavy-ion collisions.* Nucl. Phys. A **517** (1990) 615.

[68] M. I. Abdulhamid et al. Measurements of dielectron production in Au+Au collisions at sNN=27, 39, and 62.4 GeV from the STAR experiment. *Phys. Rev. C*, 107(6):L061901, 2023.

[69] L. Adamczyk et al. Measurements of Dielectron Production in Au+Au Collisions at $\sqrt{s_{\mathrm{NN}}} = 200$ GeV from the STAR Experiment. *Phys. Rev. C*, 92(2):024912, 2015.

[70] Taesoo Song, Hamza Berrehrah, Daniel Cabrera, Juan M. Torres-Rincon, Laura Tolos, Wolfgang Cassing, and Elena Bratkovskaya. Tomography of the Quark-Gluon-Plasma by Charm Quarks. *Phys. Rev. C*, 92(1):014910, 2015.

[71] Taesoo Song, Hamza Berrehrah, Daniel Cabrera, Wolfgang Cassing, and Elena Bratkovskaya. Charm production in Pb + Pb collisions at energies available at the CERN Large Hadron Collider. *Phys. Rev. C*, 93(3):034906, 2016.

[72] Taesoo Song, Hamza Berrehrah, Juan M. Torres-Rincon, Laura Tolos, Daniel Cabrera, Wolfgang Cassing, and Elena Bratkovskaya. Single electrons from heavy-flavor mesons in relativistic heavy-ion collisions. *Phys. Rev. C*, 96(1):014905, 2017.